

Power and limitations of distributed quantum state purification

Benchi Zhao,¹ Yu-Ao Chen,² Xuanqiang Zhao,¹ Chengkai Zhu,² Giulio Chiribella,^{1,3,4,*} and Xin Wang^{2,†}

¹*QICI Quantum Information and Computation Initiative, School of Computing and Data Science, The University of Hong Kong, Pokfulam Road, Hong Kong*

²*Thrust of Artificial Intelligence, Information Hub, The Hong Kong University of Science and Technology (Guangzhou), Guangdong 511453, China*

³*Quantum Group, Department of Computer Science, University of Oxford, Wolfson Building, Parks Road, Oxford, OX1 3QD, United Kingdom*

⁴*Perimeter Institute for Theoretical Physics, 31 Caroline Street North, Waterloo, Ontario, Canada*

Quantum state purification protocols, which mitigate noise by converting multiple copies of noisy quantum states into fewer copies with a lower noise level, have applications in quantum communication and computation with imperfect devices. Here, we systematically study the task of state purification in distributed quantum systems, demanding that purification be achieved by local operations and classical communication (LOCC). We prove that, in the presence of depolarizing noise, no LOCC purification protocol starting from two copies can work blindly for all the states in three important sets: the set of all pure two-qubit states, the set of all two-qubit maximally entangled states, and the Bell basis. In stark contrast, we show that a targeted, single-state purification is always achievable in the presence of depolarizing noise, and we provide an explicit analytical LOCC protocol for every given two-qubit state. For arbitrary finite sets of pure states and arbitrary noise profiles, we develop an optimization-based algorithm that systematically designs LOCC purification protocols, and we demonstrate it through concrete examples. Overall, our results identify both fundamental limitations and practical noise reduction strategies for distributed quantum information processing.

Introduction.— Quantum computers promise major speedups in certain computational problems, and are expected to impact a broad range of areas, including cryptography [1, 2], machine learning [3, 4], and quantum chemistry [5, 6]. However, the number of qubits in existing hardware implementations is still limited, thereby preventing the solution of practically relevant problems. For example, the largest superconducting processors have several hundreds of physical qubits [7], while solving real-world problems such as factoring RSA numbers requires millions of qubits [8].

Distributed quantum computing (DQC) [9–12] offers a promising route to scale up the size of quantum computations. The idea is to combine the power of multiple quantum processors, by letting them perform joint computations via local operations and classical communication (LOCC) [13], which is essential for entanglement distillation [14–17] and distribution [18–21] in quantum networks. While individual processors have limited capacity, the total power of the overall network can facilitate the implementation of advanced quantum algorithms [22, 23].

A remaining challenge, however, is the presence of noise and decoherence, which limits the performance of all realistic quantum computing architectures, including DQC. In practice, quantum systems inevitably interact with their environment, leading to deviations from the ideal scenario of pure states and unitary dynamics. Such deviations impair the computation and limit the accuracy. To address this problem, several approaches have been developed, including quantum error correction [24–27] and error mitigation [28–32].

These approaches are designed to work in scenarios where a single copy of the noisy quantum state is available. When

multiple copies are available, instead, it is sometimes possible to remove part of the noise through quantum state purification [33–37]. Formally, a quantum state purification scenario is modelled as follows: a noisy process, described by a completely positive trace preserving (CPTP) map \mathcal{N} (also known as a quantum channel), degrades a pure state $\psi = |\psi\rangle\langle\psi|$ into a mixed state $\mathcal{N}(\psi)$ [38]. Then, the purification protocol is applied to approximately restore the initial pure state; mathematically, the protocol is described by a completely positive trace non-increasing (CPTN) map \mathcal{E} (also known as a quantum operation) that probabilistically yields a higher-fidelity state $\sigma_\psi = \mathcal{E}(\mathcal{N}(\psi)^{\otimes n}) / \text{Tr}[\mathcal{E}(\mathcal{N}(\psi)^{\otimes n})]$ from n noisy copies of the noisy state $\mathcal{N}(\psi)$. The condition for a purification protocol to be useful is that the final state σ_ψ has a higher fidelity to the initial state ψ than the noisy state $\mathcal{N}(\psi)$; in formula, $F(\sigma_\psi, \psi) \geq F(\mathcal{N}(\psi), \psi)$, where $F(\rho, \sigma) := \|\sqrt{\rho}\sqrt{\sigma}\|_1^2$ denotes quantum fidelity. If the target state ψ is known, the purification is called *targeted state purification*, e.g., entanglement distillation [14–17] and magic state distillation [39–41]. For a more general setting, if the target state ψ is unknown and is drawn from a state set \mathcal{S} , the purification is called *blind state purification*.

Most existing purification protocols have considered a global setting, in which arbitrary joint operations are allowed on the n -copy state [33–37] (see the Supplemental Material A for more discussion). In DQC, it is important to consider a scenario where the state ψ and its noisy version $\mathcal{N}(\psi)$ are distributed to multiple processors. As illustrated in FIG. 1, these processors have access only to the assigned subsystems and are restricted to performing LOCC. Until now, however, this scenario has remained largely unexplored. Is it possible to find distributed purification protocols that purify quantum states using only LOCC? Is quantum entanglement an essential resource for purifying noisy quantum states?

In this work, we investigate the feasibility of distributed

* giulio@cs.hku.hk

† felixxinwang@hkust-gz.edu.cn

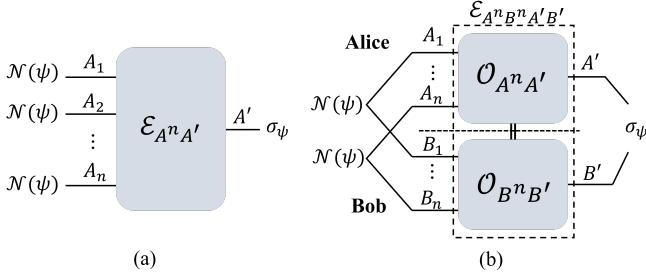


FIG. 1. Diagram of $n \rightarrow 1$ purification protocol. (a) Global purification protocol with $\mathcal{E}_{A^n A'} \in \text{CPTN}$. (b) Distributed purification protocol with $\mathcal{E}_{A^n B^n A' B'} \in \text{LOCC} \cap \text{CPTN}$.

blind state purification under depolarizing noise, which is a canonical quantum noise process defined as $\mathcal{N}^\gamma(\psi) = (1 - \gamma)\psi + \gamma \frac{I}{d}$, where γ denotes the noise level, I is the identity matrix, and d is the Hilbert space dimension. Specifically, we consider the scenario where an unknown state ψ is drawn from the set \mathcal{S}_P of all pure states or from the set \mathcal{S}_B of four Bell states, and the noisy state $\mathcal{N}^\gamma(\psi)$ is shared between remote parties. We show that no nontrivial $2 \rightarrow 1$ LOCC purification protocol exists in this setting for either set. Based on the no-go theorem for the Bell states set, similarly, we arrive at the no-go theorem for the maximally entangled states set \mathcal{S}_{MES} . Importantly, these $2 \rightarrow 1$ no-go results do not extend to the general $n \rightarrow 1$ setting since, given many copies of the noisy state $\mathcal{N}^\gamma(\psi)$, the remote parties could implement tomography to determine the state. Then, the problem reduces to purifying a known quantum state with LOCC, i.e., targeted state purification. Notably, when the target state is the Bell state, the task reduces to entanglement distillation [14, 17, 42, 43]. For an arbitrary given state, we construct an analytical $2 \rightarrow 1$ LOCC purification protocol. For the state sets with finite size, we further introduce an optimization-based algorithm for designing LOCC purification protocols. These results establish fundamental limitations and constructive methods for distributed state purification, offering a new avenue for reducing noise in distributed quantum architectures.

No-go theorem for distributed purification protocol.— We start with some notations. Denote a pure state as $|\psi\rangle$, and the corresponding density matrix is denoted as $\psi = |\psi\rangle\langle\psi|$. The Bell states are defined as $|\Phi\rangle^\pm = \frac{1}{\sqrt{2}}(|00\rangle \pm |11\rangle)$, and $|\Psi\rangle^\pm = \frac{1}{\sqrt{2}}(|01\rangle \pm |10\rangle)$, with corresponding Bell density matrices Φ^\pm, Ψ^\pm , respectively. The distributed $n \rightarrow 1$ purification protocol is denoted as $\mathcal{E}_{A^n B^n A' B'}$, where $A^n B^n = A_1 B_1 A_2 B_2 \cdots A_n B_n$ is the input system, and $A' B'$ is the output system. In this work, we only consider the case of 2-qubit systems.

Suppose we have a noisy state $\mathcal{N}(\psi)$, where ψ is some pure state and \mathcal{N} is a given noise channel. Let \mathcal{E} be an $n \rightarrow 1$ CPTN-LOCC map. Then the output state is

$$\sigma_\psi := \frac{\tilde{\sigma}_\psi}{p_\psi} = \frac{\mathcal{E}(\mathcal{N}(\psi)^{\otimes n})}{\text{Tr}[\mathcal{E}(\mathcal{N}(\psi)^{\otimes n})]}, \quad (1)$$

where $\tilde{\sigma}_\psi = \mathcal{E}(\mathcal{N}(\psi)^{\otimes n})$ stands for the unnormalized output

state, and $p_\psi = \text{Tr}[\tilde{\sigma}_\psi]$ is the success probability of getting the state σ_ψ . If the output state σ_ψ is closer to the target state ψ , i.e., $F(\sigma_\psi, \psi) \geq F(\mathcal{N}(\psi), \psi)$, then the CPTN-LOCC map \mathcal{E} is a *distributed purification protocol* for the pure state ψ over noise \mathcal{N} . If the state ψ is sampled from a set of bipartite pure states \mathcal{S} , and the map \mathcal{E} can increase the fidelity for every state ψ in the set \mathcal{S} , then we say the CPTN-LOCC map \mathcal{E} is a *distributed purification protocol* for the set \mathcal{S} over noise \mathcal{N} . The formal definition is given in the following.

Definition 1 (Distributed purification protocol) An $n \rightarrow 1$ CPTN map \mathcal{E} is a *distributed purification protocol* for the state set \mathcal{S} over a noisy channel \mathcal{N} if the protocol \mathcal{E} can be realized by LOCC and increases the fidelity for every state in the set \mathcal{S} , i.e.,

$$F(\psi, \sigma_\psi) \geq F(\psi, \mathcal{N}(\psi)), \quad \forall \psi \in \mathcal{S}. \quad (2)$$

There is a special case called *trivial distributed purification protocol*, which refers to the protocol that preserves the fidelity for every state in the set, i.e., $F(\sigma_\psi, \psi) = F(\mathcal{N}(\psi), \psi)$, $\forall \psi \in \mathcal{S}$. For example, the partial trace channel is a trivial purification protocol. On the contrary, the *nontrivial purification protocol* is defined as a purification protocol that can strictly increase the fidelity over some states, which is $F(\sigma_\psi, \psi) > F(\mathcal{N}(\psi), \psi)$, $\exists \psi \in \mathcal{S}$. Obviously, for a given state set \mathcal{S} and a noisy channel \mathcal{N} , the $n \rightarrow 1$ distributed purification protocol \mathcal{E} is not unique, and different protocols have different performances. To fairly compare the purification protocols, we define the *average purification fidelity* to quantify the performance of different purification protocols, which only takes the successful cases into account. Specifically, sample quantum states from the state set uniformly, apply the purification protocol, rule out all the failure cases, and the average fidelity of the successful cases can be computed by $\bar{F}(n; \mathcal{S}, \mathcal{N}, \mathcal{E}) = \frac{1}{|\mathcal{S}|} \sum_{\psi \in \mathcal{S}} F(\psi, \frac{\tilde{\sigma}_\psi}{\bar{P}})$, where $\tilde{\sigma}_\psi$ is the unnormalized purified state, and \bar{P} is the average successful probability. Clearly, the performance of a purification protocol depends on the average successful probability \bar{P} . Thus, with a given average success probability \bar{P} , we define the *optimal distributed purification protocol* \mathcal{E}^* as a protocol that achieves the *optimal average purification fidelity*, which is

$$\begin{aligned} \bar{F}_{\text{LOCC}}^*(n, \bar{P}; \mathcal{S}, \mathcal{N}) &= \bar{F}(n; \mathcal{S}, \mathcal{N}, \mathcal{E}^*) \\ &= \max_{\mathcal{E}} \left\{ \bar{F}(n; \mathcal{S}, \mathcal{N}, \mathcal{E}) \mid \mathcal{E} \in \text{LOCC} \cap \text{CPTN}, \right. \\ &\quad \left. \frac{1}{|\mathcal{S}|} \sum_{\psi \in \mathcal{S}} \text{Tr}[\mathcal{E}(\mathcal{N}(\psi)^{\otimes n})] = \bar{P} \right\}. \quad (3) \end{aligned}$$

The definition of average purification fidelity is also valid for the continuous state set by replacing the summation with the integral. Details can be found in Supplemental Material B.

From the definition, the performance of distributed purification protocols depends on the state set. We firstly consider the universal set, which contains all 2-qubit pure states \mathcal{S}_P . Surprisingly, our first main result reveals that there does not exist a $2 \rightarrow 1$ nontrivial distributed purification protocol.

Theorem 1 (No-go theorem for the pure state set) *For the depolarizing noise channel \mathcal{N}_{AB}^γ with noise level $\gamma \in (0, 1)$, there is no nontrivial $2 \rightarrow 1$ LOCC purification protocol for the set \mathcal{S}_P that contains all 2-qubit pure states.*

To prove Theorem 1, we first relax LOCC to positive partial transpose (PPT) operations. Then we assume there exists a non-trivial purification protocol \mathcal{E} , which must satisfy the linear constraints shown in Eq. (C3) in the Supplemental Material C. By utilizing the symmetry property of the state set \mathcal{S}_P and Schur's lemma, we reform and simplify the linear constraints, and the problem becomes an SDP problem. We then prove that the optimal solution to the SDP corresponds to the trivial purification protocol, implying there is no non-trivial distributed purification protocol. The proof is shown in the Supplemental Material C.

Here, we would like to emphasize that the $2 \rightarrow 1$ no-go theorem for the pure state set \mathcal{S}_P does not imply the $n \rightarrow 1$ no-go theorem. For a straightforward strategy, if two parties share infinitely many copies of the noisy state $\mathcal{N}^\gamma(\psi)$, where ψ is an arbitrary pure state, they could implement tomography to obtain the density matrix of the noisy state. Since the noisy channel \mathcal{N}^γ is global depolarizing noise, $\mathcal{N}^\gamma(\psi) = (1-\gamma)\psi + \gamma \frac{I}{4}$, the two parties can deduce the pure state ψ from the density matrix of the noisy state. Now the problem reduces to purifying a known quantum state with a distributed purification protocol. Such a problem will be demonstrated in the next section.

The proof of Theorem 1 is highly dependent on the symmetry of the pure state set \mathcal{S}_P . It is natural to ask whether a nontrivial distributed protocol exists if we consider a less symmetric state set. Here we take the Bell state set \mathcal{S}_B into consideration, i.e., $\mathcal{S}_B = \{\Phi^+, \Phi^-, \Psi^+, \Psi^-\}$. In DQC, operations are applied to the quantum systems locally, and thus it is natural to assume the noise is introduced locally, e.g., a bi-local depolarizing noise $\mathcal{N}_{AB}^{\gamma_1, \gamma_2} = \mathcal{N}_A^{\gamma_1} \otimes \mathcal{N}_B^{\gamma_2}$, which is equivalent to a global noise $\mathcal{N}_{AB}^{\gamma'}$ with parameter $\gamma' = 1 - (1 - \gamma_1)(1 - \gamma_2)$ shown in Supplemental Material F. Notably, for \mathcal{S}_B and $\mathcal{N}_{AB}^{\gamma_1, \gamma_2}$, we show that a non-trivial purification protocol still does not exist.

Theorem 2 (No-go theorem for four Bell states) *For the bi-local depolarizing noise channel $\mathcal{N}_{AB}^{\gamma_1, \gamma_2}$ with noise levels γ_1 and γ_2 , there is no nontrivial $2 \rightarrow 1$ LOCC purification protocol for the set \mathcal{S}_B that contains 4 Bell states.*

The detailed proof is shown in Supplemental Material G. By Theorem 2, there does not exist a $2 \rightarrow 1$ distributed blind purification protocol \mathcal{E} that can increase the fidelity for four Bell states simultaneously. However, if we only care about one Bell state rather than four, then the problem reduces to entanglement distillation, and it is possible to increase the fidelity with a purification protocol.

If we apply the local unitaries $W_{AB} = U_A \otimes V_B$ to the Bell states set, we could obtain a new set $\mathcal{S}_B^{W_{AB}}$. Since the local unitary transformed set is equivalent to the Bell states set, we could arrive at the following corollary.

Corollary 3 *For the bi-local depolarizing noise channel $\mathcal{N}_{AB}^{\gamma_1, \gamma_2}$ with noise levels γ_1 and γ_2 , there is no nontrivial $2 \rightarrow 1$ LOCC purification protocol for the set $\mathcal{S}_B^{W_{AB}}$ that contains 4 arbitrary orthogonal maximally entangled states.*

Combining Theorem 2 and Corollary 3, it is straightforward to arrive at a statement that there does not exist a non-trivial $2 \rightarrow 1$ purification protocol for the union set $\mathcal{S}_U = \mathcal{S}_B \cup \mathcal{S}_B^{W_{AB}^1} \cup \dots \cup \mathcal{S}_B^{W_{AB}^k} \dots \cup \mathcal{S}_B^{W_{AB}^n}$, where W_{AB}^k refers to local unitary operation. If there exists a nontrivial $2 \rightarrow 1$ purification protocol for the union set \mathcal{S}_U , it means the purified fidelity strictly increases for some states, i.e., $F(\psi, \sigma_\psi) > F(\psi, \mathcal{N}(\psi))$, $\exists \psi \in \mathcal{S}_U$. Then, by removing some states from the union set, we obtain $F(\psi, \sigma_\psi) > F(\psi, \mathcal{N}(\psi))$, $\exists \psi \in \mathcal{S}_B^{W_{AB}^k}$, which contradicts the no-go theorem shown in Corollary 3. Therefore, there must be no nontrivial purification protocol for the union set \mathcal{S}_U . If all local unitary operations are considered, the union set becomes the maximally entangled state set

$$\begin{aligned} \mathcal{S}_{MES} &= \mathcal{S}_B \cup \mathcal{S}_B^{W_{AB}^1} \cup \dots \cup \mathcal{S}_B^{W_{AB}^k} \dots \cup \mathcal{S}_B^{W_{AB}^\infty} \\ &= \{|\Phi\rangle\langle\Phi| \mid |\Phi\rangle = U_A \otimes V_B |\Phi^+\rangle, \forall U_A, V_B \in SU(2)\}, \end{aligned}$$

and we arrive at the no-go theorem for maximally entangled states set \mathcal{S}_{MES} .

Corollary 4 (No-go theorem for maximally entangled states set) *For the local depolarizing noise channel $\mathcal{N}_{AB}^{\gamma_1, \gamma_2}$ with noise levels γ_1 and γ_2 , there is no nontrivial $2 \rightarrow 1$ LOCC purification protocol for the set \mathcal{S}_{MES} that contains all maximally entangled pure states.*

The above no-go theorems highlight the essential role of entanglement in quantum state purification. Without entanglement, LOCC alone is not sufficiently powerful to purify these representative sets of quantum states.

Purifying a known state with LOCC protocol.— We have seen different no-go theorems for the distributed state purification. Then what can we do if we know more information about the noisy states? The simplest case is that the state set \mathcal{S} only has one pure state $|\mathcal{S}| = 1$ and the state is known. This case is trivial in the global purification setting, because the global purification protocol can directly prepare the target state ψ . However, such a problem is nontrivial in the distributed computing paradigm, as it is impossible to prepare the state ψ via an LOCC protocol as long as ψ is entangled. In Theorem 5, we show that a nontrivial distributed purification protocol exists if the target state ψ is known.

Theorem 5 (Distributed purification protocol for known states) *For a given pure state ψ , which is corrupted by the bi-local depolarizing noise channel $\mathcal{N}_{AB}^{\gamma}$ with noise level $\gamma \in [0, 0.4]$, there always exists a nontrivial LOCC purification protocol, such that the purified state σ_ψ has a strictly higher fidelity, i.e., $F(\sigma_\psi, \psi) > F(\mathcal{N}_{AB}^{\gamma}(\psi), \psi)$.*

To prove the theorem, we propose an analytical $2 \rightarrow 1$ distributed purification protocol to purify the state corrupted

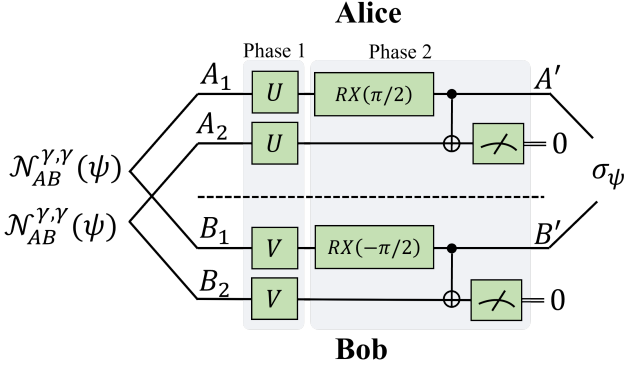


FIG. 2. Diagram for the $2 \rightarrow 1$ analytical distributed purification protocol for noisy state $\mathcal{N}_{AB}^{\gamma,\gamma}(\psi)$. This purification protocol has two phases. In phase 1, the local unitaries map the noisy state $\mathcal{N}_{AB}^{\gamma,\gamma}(\psi)$ to $\mathcal{N}_{AB}^{\gamma,\gamma}(\psi_\alpha)$. Phase 2 can purify the noisy state $\mathcal{N}_{AB}^{\gamma,\gamma}(\psi_\alpha)$ for arbitrary $\alpha \in [0, 1]$.

by bi-local depolarizing noise, which is shown in FIG. 2. When two parties, Alice and Bob, possess two copies of shared noisy states $\mathcal{N}_{AB}^{\gamma,\gamma}(\psi)$, they apply some local unitaries U and V on their own systems respectively (as shown in Phase 1), mapping the noisy state $\mathcal{N}_{AB}^{\gamma,\gamma}(\psi)$ to $\mathcal{N}_{AB}^{\gamma,\gamma}(\psi_\alpha)$, where $|\psi_\alpha\rangle = \alpha|00\rangle + \sqrt{1-\alpha^2}|11\rangle$ with $\alpha \in [0, 1]$. Then, for the noisy state $\mathcal{N}_{AB}^{\gamma,\gamma}(\psi_\alpha)$ with arbitrary $\alpha \in [0, 1]$, the circuit shown in Phase 2 can non-trivially purify it. Specifically, Alice and Bob apply local rotation gates and CNOT gates on their own parts, and make measurements on systems A_2, B_2 . Denote the measurement results as m_A and m_B respectively, and Alice and Bob exchange the results via classical communication. If $m_A = m_B = 0$, then the purification is successful and outputs the purified state σ_ψ ; otherwise, the purification fails and the process described above needs to be repeated. To verify the effectiveness of the proposed protocol, we derive the fidelity of the purified state and the target state $F(\sigma_\psi, \psi)$ and show that $F(\sigma_\psi, \psi) - F(\mathcal{N}_{AB}^{\gamma,\gamma}(\psi), \psi) \geq 0$ holds for arbitrary states with $\gamma \in [0, 0.4]$. Here we would like to highlight that the protocol shown in FIG. 2 not only can purify a single state, but also works for a set of states with the same Schmidt basis. More details are shown in Supplemental Material H.

The conventional distributed purification protocols, such as DEJMPS [42] and BBPSSW[14], can only purify the noisy maximally entangled state. While the proposed protocol, as shown in FIG. 2, can not only purify maximally entangled states, but also works for non-maximally entangled states. Note that non-maximally entangled states are also important resources in distributed quantum information processing tasks such as entanglement catalyst [44] and the verification of Hardy's paradox [45, 46].

Purification protocol via optimization.— In a more general case, where the state set contains more than one pure state, i.e., $|\mathcal{S}| \geq 2$, the proposed protocol shown in FIG. 2 no longer works, and we have to propose an LOCC purification protocol for every new state set. This motivates us to introduce an automatic algorithm to design the distributed purification proto-

col. Specifically, Alice and Bob share n copies of noisy states $\mathcal{N}_{AB}(\psi)$, and the state ψ is sampled from a set of pure states \mathcal{S} . Alice and Bob apply local unitaries U and V on their own systems, respectively. After measuring all the systems except the first pair, the two parties check the measurement results via classical communication. If the measurement results are all 0, the purification process is successful, and the first pair state is the purified state σ_ψ ; otherwise, the purification fails.

In this algorithm, the optimal local unitaries U and V , that satisfy the constraints, are unknown. To solve this problem, we utilize the parametrized quantum circuits (PQCs) [47] to represent the local unitaries $U(\theta)$ and $V(\zeta)$, and apply gradient-based optimization method [48] to search the optimal parameters θ, ζ in the PQCs $U(\theta)$ and $V(\zeta)$. The optimization method has been successfully applied to various tasks, such as quantum chemistry [49–52], quantum information analysis [17, 53–56], and quantum data compression [57, 58]. Note that the optimized protocols here no longer require the noise level constraint $\gamma \leq 0.4$, a condition needed in Theorem 5 for nontrivial purification.

To optimize the parameters in the PQCs, we have to design a cost function that describes our requirements. In the case of a distributed purification protocol, there are two requirements. For the first one, the average of purified fidelity should be as large as possible, i.e., $\max_{U,V} \sum_{\psi \in \mathcal{S}} F(\psi, \sigma_\psi)$. For the second one, the purification protocol should increase the fidelity for every purified state in the set, i.e., $F(\psi, \sigma_\psi) \geq F(\psi, \mathcal{N}(\psi))$, $\forall \psi \in \mathcal{S}$. Based on the requirements, we have the following cost function

$$C = - \sum_{\psi \in \mathcal{S}} F(\psi, \sigma_\psi) + \sum_{\psi \in \mathcal{S}} S(F(\psi, \mathcal{N}(\psi)) - F(\psi, \sigma_\psi)), \quad (4)$$

where $S(x) = \frac{1}{1+e^{-ax}}$ is sigmoid function with positive real coefficient a . The first summation term $\sum_{\psi \in \mathcal{S}} F(\psi, \sigma_\psi)$ corresponds to the first requirement. The second summation is the punishment term. When $F(\psi, \mathcal{N}(\psi)) - F(\psi, \sigma_\psi) \geq 0$, it implies the purified state has lower fidelity, then $S(F(\psi, \mathcal{N}(\psi)) - F(\psi, \sigma_\psi)) \geq 1/2$. The more the fidelity drops, the greater the punishment will be. The penalty strength can be modified by tuning the parameter a . With the chosen ansatz and the cost function Eq. (4), we can execute the optimization algorithm to train the parameters. More algorithm details please refer to the Supplemental Material I.

Here we conduct numerical experiments [59], via the QUAIRKIT platform [60], to show the effectiveness of the optimized purification protocol. The numerical results are shown in FIG. 3. Specifically, we consider the pure state set containing 4 different states $\mathcal{S}_d = \{\psi_{\frac{1}{\sqrt{2}}}, \psi_{\frac{1}{\sqrt{3}}}, \psi_{\frac{1}{\sqrt{4}}}, \psi_{\frac{1}{\sqrt{5}}}\}$, where $|\psi_\alpha\rangle = \alpha|00\rangle + \sqrt{1-\alpha^2}|11\rangle$. The noise model is bi-local depolarizing channel $\mathcal{N}_{AB}^{\gamma,\gamma}$, with noise level varying $\gamma \in [0, 0.4]$. From the proof of Theorem 5, the Phase 2 circuit shown in FIG. 2 is a nontrivial purification protocol for the state in the form of $|\psi_\alpha\rangle$. Thus, the Phase 2 circuit can also non-trivially purify the set \mathcal{S}_d . We compare the performance of the optimized protocol and the analytical protocol and find that the optimized protocol achieves higher fidelity. To bench-

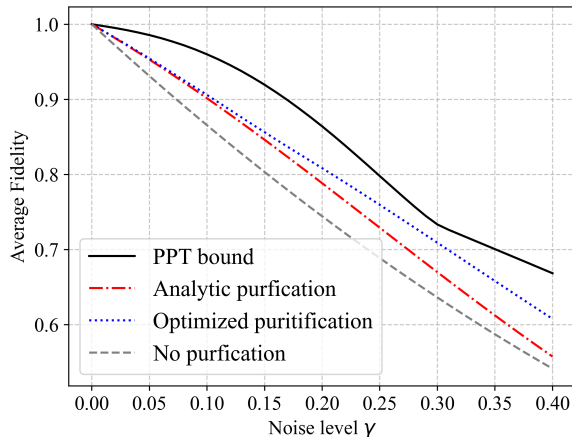


FIG. 3. Comparison of the performance of different $2 \rightarrow 1$ distributed purification protocols. The black solid line is the PPT upper bound. The dotted blue line is achieved by the optimized purification protocol. The dash-dot red curve corresponds to the Phase 2 circuit shown in FIG. 2. The dashed grey line refers to the fidelity without purification.

mark the performance of the optimized purification protocol, we compare the fidelity achieved by the optimized purification protocol and the PPT bound, which is calculated by the SDP shown in Supplemental Material E. Here, we fix the average success probability as 0.1. Note that the fidelity achieved by optimized purification is close to the PPT bound, implying the performance of the optimized purification is remarkable. For larger quantum noise level, the average fidelity becomes more complicated, and we include it in the Supplemental Material J. We also conduct more numerical experiments for better understanding (cf. Supplemental Material K).

Discussion.— In this work, we systematically characterized the fundamental limitations and operational capabilities

of distributed state purification. In particular, we proved that, in the presence of depolarizing noise, no $2 \rightarrow 1$ LOCC purification protocol can work blindly for all states in three important sets: the set of all pure two-qubit states, the set of all two-qubit maximally entangled states, and the Bell basis. If instead the purification protocol is targeted to a single, known pure state, an explicit purification protocol can be constructed. Finally, for a finite set of pure states, we introduced an optimization-based algorithm to design LOCC purification protocols. These results identify both no-go regimes and constructive possibilities, establishing distributed state purification as a viable strategy for enhancing noise resilience in quantum networks.

For future work, it would be interesting to identify the necessary and sufficient conditions for state sets that admit a non-trivial distributed purification protocol, and it would also be important to figure out how the symmetry of noise relates to the no-go theorems. Another promising direction is to determine the optimal $n \rightarrow 1$ purification protocol under LOCC constraints, as well as to study the power and limitations under the multipartite entanglement regime.

Acknowledgements— B.Z. and X.W. would like to thank Jiayi Zhao and Bartosz Regula for insightful discussions. G.C. and X.Z. acknowledge support from the Chinese Ministry of Science and Technology (MOST) through grant 2023ZD0300600, by the Hong Kong Research Grant Council (RGC) through grant R7035-21F, and by the State Key Laboratory of Quantum Information Technologies and Materials, Chinese University of Hong Kong. X.W. acknowledges the support from the National Natural Science Foundation of China (Grant No. 12447107), the Guangdong Provincial Quantum Science Strategic Initiative (Grant No. GDZX2403008, GDZX2503001), the Guangdong Natural Science Foundation (Grant No. 2025A1515012834), and the Quantum Science Center of Guangdong-Hong Kong-Macao Greater Bay Area.

-
- [1] P. W. Shor, Polynomial-time algorithms for prime factorization and discrete logarithms on a quantum computer, *SIAM Review* **41**, 303 (1999).
 - [2] R. L. Rivest, A. Shamir, and L. Adleman, A method for obtaining digital signatures and public-key cryptosystems, *Communications of the ACM* **21**, 120 (1978).
 - [3] J. Biamonte, P. Wittek, N. Pancotti, P. Rebentrost, N. Wiebe, and S. Lloyd, Quantum machine learning, *Nature* **549**, 195 (2017).
 - [4] S. Lloyd, M. Mohseni, and P. Rebentrost, Quantum principal component analysis, *Nature Physics* **10**, 631 (2014).
 - [5] R. P. Feynman, Simulating physics with computers, in *Feynman and computation* (cRC Press, 2018) pp. 133–153.
 - [6] Y. Cao, J. Romero, J. P. Olson, M. Degroote, P. D. Johnson, M. Kieferová, I. D. Kivlichan, T. Menke, B. Peropadre, N. P. Sawaya, et al., Quantum chemistry in the age of quantum computing, *Chemical Reviews* **119**, 10856 (2019).
 - [7] Quantum error correction below the surface code threshold, *Nature* **638**, 920 (2025).
 - [8] C. Gidney, How to factor 2048 bit rsa integers with less than a million noisy qubits, *arXiv preprint arXiv:2505.15917* (2025).
 - [9] M. Caleffi, M. Amoretti, D. Ferrari, J. Illiano, A. Manzalini, and A. S. Cacciapuoti, Distributed quantum computing: a survey, *Computer Networks* **254**, 110672 (2024).
 - [10] T. Peng, A. W. Harrow, M. Ozols, and X. Wu, Simulating large quantum circuits on a small quantum computer, *Physical Review Letters* **125**, 150504 (2020).
 - [11] K. Mitarai and K. Fujii, Constructing a virtual two-qubit gate by sampling single-qubit operations, *New Journal of Physics* **23**, 023021 (2021).
 - [12] C. Piveteau and D. Sutter, Circuit knitting with classical communication, *IEEE Transactions on Information Theory* **70**, 2734 (2023).
 - [13] E. Chitambar, D. Leung, L. Mančinska, M. Ozols, and A. Winter, Everything you always wanted to know about locc (but were afraid to ask), *Communications in Mathematical Physics* **328**, 303 (2014).
 - [14] C. H. Bennett, G. Brassard, S. Popescu, B. Schumacher, J. A.

- Smolin, and W. K. Wootters, Purification of noisy entanglement and faithful teleportation via noisy channels, *Physical Review Letters* **76**, 722 (1996).
- [15] I. Devetak and A. Winter, Distillation of secret key and entanglement from quantum states, *Proceedings of the Royal Society A: Mathematical, Physical and Engineering Sciences* **461**, 207 (2005), arXiv:0306078 [quant-ph].
- [16] K. Fang, X. Wang, M. Tomamichel, and R. Duan, Non-Asymptotic Entanglement Distillation, *IEEE Transactions on Information Theory* **65**, 10.1109/TIT.2019.2914688 (2019).
- [17] X. Zhao, B. Zhao, Z. Wang, Z. Song, and X. Wang, Practical distributed quantum information processing with loccnet, *npj Quantum Information* **7**, 159 (2021).
- [18] H.-J. Briegel, W. Dür, J. I. Cirac, and P. Zoller, Quantum Repeaters: The Role of Imperfect Local Operations in Quantum Communication, *Physical Review Letters* **81**, 5932 (1998), arXiv:9803056v1 [quant-ph].
- [19] W. Dür, H.-J. Briegel, J. I. Cirac, and P. Zoller, Quantum repeaters based on entanglement purification, *Physical Review A* **59**, 169 (1999), arXiv:9808065 [quant-ph].
- [20] K. Azuma, K. Tamaki, and H.-K. Lo, All-photonic quantum repeaters, *Nature Communications* **6**, 6787 (2015), arXiv:1309.7207.
- [21] Y.-A. Chen, X. Liu, C. Zhu, L. Zhang, J. Liu, and X. Wang, Quantum Entanglement Allocation through a Central Hub, arXiv preprint arXiv:2409.08173 (2024).
- [22] K. Fujii, K. Mizuta, H. Ueda, K. Mitarai, W. Mizukami, and Y. O. Nakagawa, Deep variational quantum eigensolver: a divide-and-conquer method for solving a larger problem with smaller size quantum computers, *PRX Quantum* **3**, 010346 (2022).
- [23] Z. Zhou, Y. Du, X. Tian, and D. Tao, Qaoa-in-qaoa: solving large-scale maxcut problems on small quantum machines, *Physical Review Applied* **19**, 024027 (2023).
- [24] E. Knill and R. Laflamme, Theory of quantum error-correcting codes, *Physical Review A* **55**, 900 (1997).
- [25] A. R. Calderbank and P. W. Shor, Good quantum error-correcting codes exist, *Physical Review A* **54**, 1098 (1996).
- [26] E. Knill, R. Laflamme, and L. Viola, Theory of quantum error correction for general noise, *Physical Review Letters* **84**, 2525 (2000).
- [27] R. Chao and B. W. Reichardt, Quantum error correction with only two extra qubits, *Physical Review Letters* **121**, 050502 (2018).
- [28] K. Temme, S. Bravyi, and J. M. Gambetta, Error mitigation for short-depth quantum circuits, *Physical Review Letters* **119**, 180509 (2017).
- [29] Z. Cai, R. Babbush, S. C. Benjamin, S. Endo, W. J. Huggins, Y. Li, J. R. McClean, and T. E. O'Brien, Quantum error mitigation, *Reviews of Modern Physics* **95**, 045005 (2023).
- [30] S. Endo, S. C. Benjamin, and Y. Li, Practical quantum error mitigation for near-future applications, *Physical Review X* **8**, 031027 (2018).
- [31] B. Zhao, M. Jing, L. Zhang, X. Zhao, Y.-A. Chen, K. Wang, and X. Wang, Retrieving nonlinear features from noisy quantum states, *PRX Quantum* **5**, 020357 (2024).
- [32] X. Zhao, B. Zhao, Z. Xia, and X. Wang, Information recoverability of noisy quantum states, *Quantum* **7**, 978 (2023).
- [33] J. Fiurášek, Optimal probabilistic cloning and purification of quantum states, *Physical Review A—Atomic, Molecular, and Optical Physics* **70**, 032308 (2004).
- [34] H. Yao, Y.-A. Chen, E. Huang, K. Chen, H. Fu, and X. Wang, Protocols and trade-offs of quantum state purification, *Quantum Science and Technology* **10**, 035020 (2025).
- [35] J. I. Cirac, A. Ekert, and C. Macchiavello, Optimal purification of single qubits, *Physical Review Letters* **82**, 4344 (1999).
- [36] A. Barenco, A. Berthiaume, D. Deutsch, A. Ekert, R. Jozsa, and C. Macchiavello, Stabilization of quantum computations by symmetrization, *SIAM Journal on Computing* **26**, 1541 (1997).
- [37] A. M. Childs, H. Fu, D. Leung, Z. Li, M. Ozols, and V. Vyas, Streaming quantum state purification, *Quantum* **9**, 1603 (2025).
- [38] M. A. Nielsen and I. L. Chuang, *Quantum computation and quantum information* (Cambridge university press, 2010).
- [39] T. Itogawa, Y. Takada, Y. Hirano, and K. Fujii, Efficient magic state distillation by zero-level distillation, *PRX Quantum* **6**, 020356 (2025).
- [40] S. Bravyi and J. Haah, Magic-state distillation with low overhead, *Physical Review A—Atomic, Molecular, and Optical Physics* **86**, 052329 (2012).
- [41] P. Sales Rodriguez, J. M. Robinson, P. N. Jepsen, Z. He, C. Duckering, C. Zhao, K.-H. Wu, J. Campo, K. Bagnall, M. Kwon, et al., Experimental demonstration of logical magic state distillation, *Nature* **645**, 620 (2025).
- [42] D. Deutsch, A. Ekert, R. Jozsa, C. Macchiavello, S. Popescu, and A. Sanpera, Quantum privacy amplification and the security of quantum cryptography over noisy channels, *Physical Review Letters* **77**, 2818 (1996).
- [43] A. Zang, X. Chen, E. Chitambar, M. Suchara, and T. Zhong, No-go theorems for universal entanglement purification, *Physical Review Letters* **134**, 190803 (2025).
- [44] D. Jonathan and M. B. Plenio, Entanglement-assisted local manipulation of pure quantum states, *Physical Review Letters* **83**, 3566 (1999).
- [45] L. Hardy, Quantum mechanics, local realistic theories, and lorentz-invariant realistic theories, *Physical Review Letters* **68**, 2981 (1992).
- [46] L. Hardy, Nonlocality for two particles without inequalities for almost all entangled states, *Physical Review Letters* **71**, 1665 (1993).
- [47] M. Benedetti, E. Lloyd, S. Sack, and M. Fiorentini, Parameterized quantum circuits as machine learning models, *Quantum Science and Technology* **4**, 043001 (2019).
- [48] M. Cerezo, A. Arrasmith, R. Babbush, S. C. Benjamin, S. Endo, K. Fujii, J. R. McClean, K. Mitarai, X. Yuan, L. Cincio, et al., Variational quantum algorithms, *Nature Reviews Physics* **3**, 625 (2021).
- [49] A. Kandala, A. Mezzacapo, K. Temme, M. Takita, M. Brink, J. M. Chow, and J. M. Gambetta, Hardware-efficient variational quantum eigensolver for small molecules and quantum magnets, *Nature* **549**, 242 (2017).
- [50] A. Peruzzo, J. McClean, P. Shadbolt, M.-H. Yung, X.-Q. Zhou, P. J. Love, A. Aspuru-Guzik, and J. L. O'Brien, A variational eigenvalue solver on a photonic quantum processor, *Nature Communications* **5**, 4213 (2014).
- [51] J. R. McClean, M. E. Kimchi-Schwartz, J. Carter, and W. A. De Jong, Hybrid quantum-classical hierarchy for mitigation of decoherence and determination of excited states, *Physical Review A* **95**, 042308 (2017).
- [52] K. M. Nakanishi, K. Mitarai, and K. Fujii, Subspace-search variational quantum eigensolver for excited states, *Physical Review Research* **1**, 033062 (2019).
- [53] R. Chen, B. Zhao, and X. Wang, Near-term efficient quantum algorithms for entanglement analysis, *Physical Review Applied* **20**, 024071 (2023).
- [54] R. Chen, Z. Song, X. Zhao, and X. Wang, Variational quantum algorithms for trace distance and fidelity estimation, *Quantum Science and Technology* **7**, 015019 (2021).

- [55] B. Zhao and K. Fujii, Variational quantum hamiltonian engineering, *Physical Review Research* **7**, 023123 (2025).
- [56] X. Liu, J. Zhao, B. Zhao, and X. Wang, Dynamic locc circuits for automated entanglement manipulation, *arXiv preprint arXiv:2509.07841* (2025).
- [57] J. Romero, J. P. Olson, and A. Aspuru-Guzik, Quantum autoencoders for efficient compression of quantum data, *Quantum Science and Technology* **2**, 045001 (2017).
- [58] C. Cao and X. Wang, Noise-assisted quantum autoencoder, *Physical Review Applied* **15**, 054012 (2021).
- [59] B. Zhao, Codes for Power and limitations of distributed quantum state purification, <https://github.com/QuAIR/Entanglement-Purification-Codes> (2025).
- [60] QuAIR Team, QuAIRKit, <https://github.com/QuAIR/QuAIRKit> (2023).
- [61] D. Grinko, Mixed schur–weyl duality in quantum information, *PhD thesis* (2025).
- [62] A. Peres, Separability criterion for density matrices, *Phys. Rev. Lett.* **77**, 1413 (1996).
- [63] M. Horodecki, P. Horodecki, and R. Horodecki, Separability of n-particle mixed states: necessary and sufficient conditions in terms of linear maps, *Physics Letters A* **283**, 1 (2001).
- [64] G. E. Collins, Quantifier elimination for real closed fields by cylindrical algebraic decomposition: a synopsis, *ACM SIGSAM Bulletin* **10**, 10 (1976).
- [65] G. E. Collins, Quantifier elimination by cylindrical algebraic decomposition—twenty years of progress, *Quantifier elimination and cylindrical algebraic decomposition*, **8** (1998).
- [66] B. F. Caviness and J. R. Johnson, *Quantifier elimination and cylindrical algebraic decomposition* (Springer Science & Business Media, 2012).
- [67] G. E. Collins and H. Hong, Partial cylindrical algebraic decomposition for quantifier elimination, *Journal of Symbolic Computation* **12**, 299 (1991).
- [68] Wolfram Research, Cylindrical Decomposition, <https://reference.wolfram.com/language/ref/CylindricalDecomposition.html> (2020).
- [69] Wolfram Research, Reduce, <https://reference.wolfram.com/language/ref/Reduce.html> (2024).
- [70] Wolfram Research, Inc., *Mathematica, Version 14.3*, champaign, IL, 2025.
- [71] X. Liu, G. Liu, H.-K. Zhang, J. Huang, and X. Wang, Mitigating barren plateaus of variational quantum eigensolvers, *IEEE Transactions on Quantum Engineering* (2024).
- [72] M. Jing, E. Huang, X. Shi, S. Zhang, and X. Wang, Quantum recurrent embedding neural network, *arXiv preprint arXiv:2506.13185* (2025).
- [73] G. Vidal and C. M. Dawson, Universal quantum circuit for two-qubit transformations with three controlled-not gates, *Physical Review A* **69**, 010301 (2004).
- [74] V. V. Shende, I. L. Markov, and S. S. Bullock, Minimal universal two-qubit controlled-not-based circuits, *Physical Review A—Atomic, Molecular, and Optical Physics* **69**, 062321 (2004).

Supplemental Materials for Power and limitations of distributed quantum state purification

CONTENTS

References	5
A. Global purification protocol	8
B. Formal definitions of average purification fidelity and optimal distributed purification protocol	9
C. Proof of Theorem 1	10
D. The specific \tilde{G} in Supplemental Material C	17
E. Semidefinite program for optimal average PPT purification fidelity	19
1. Dual problem	19
F. Equivalence between global and local depolarizing noises	20
G. Proof of Theorem 2	21
H. Proof of Theorem 5	22
I. Optimized purification protocol	24
J. Distributed purification protocol for the set \mathcal{S}_d with extended noise levels	25
K. Additional numerical results	27
1. $2 \rightarrow 1$ LOCC purification protocol for sets with Bell states	27
2. $2 \rightarrow 1$ LOCC purification protocol for Bell set \mathcal{S}_B over other noise models	27
3. Comparison between optimized protocol and DEJMPS protocol	28
4. $3 \rightarrow 1$ LOCC purification protocol for the set \mathcal{S}_d over depolarizing noise	29

Supplemental Material A: Global purification protocol

The state purification has been well studied, and many practical protocols have been proposed. For example, the *symmetric projection* method [34, 36, 37] probabilistically maps the n -copy of noisy state into the symmetric subspace, and the output states have higher purity. The circuit for the implementation of symmetric projection is shown in FIG. 4. The unitary $U_k, k \in [1, n-1]$ maps the initial state $|0\rangle^{\otimes k}$ to the W-state, i.e., $U_k(|0\rangle^{\otimes k}) = \frac{1}{\sqrt{k+1}}(|00 \cdots 0\rangle + |00 \cdots 1\rangle + \cdots + |10 \cdots 0\rangle)$. Then apply control-swap gates and U_k^\dagger , then measure the ancilla qubits in the end. The measurement results are denoted as ω . If all the measurement are 0, i.e., $\omega = \mathbf{0}$, then the purification is successful and output the state $\sigma(\omega)$. Otherwise, the purification process fails, and we have to repeat the purification protocol \mathcal{E}_{sym} until it succeeds. The output purified state is

$$\sigma(\mathbf{0}) = \mathcal{E}(\mathcal{N}(\psi)^{\otimes n}) = \frac{\sum_{j=1}^n \mathcal{N}(\psi)^j}{\sum_{j=1}^n \text{Tr}[\mathcal{N}(\psi)^j]}. \quad (\text{A.1})$$

Proposition 6 For the noise channels \mathcal{N} whose dominant term of noise state $\mathcal{N}(\psi)$ remains ψ , the symmetric projection is an $n \rightarrow 1$ purification protocol for the set that contains all pure states.

Proof Since the dominant term of the noisy state $\mathcal{N}(\psi)$ remains ψ , we have

$$\mathcal{N}(\psi) = \lambda_1 \psi + \sum_{i=2}^d \lambda_i \psi_i, \quad (\text{A.2})$$

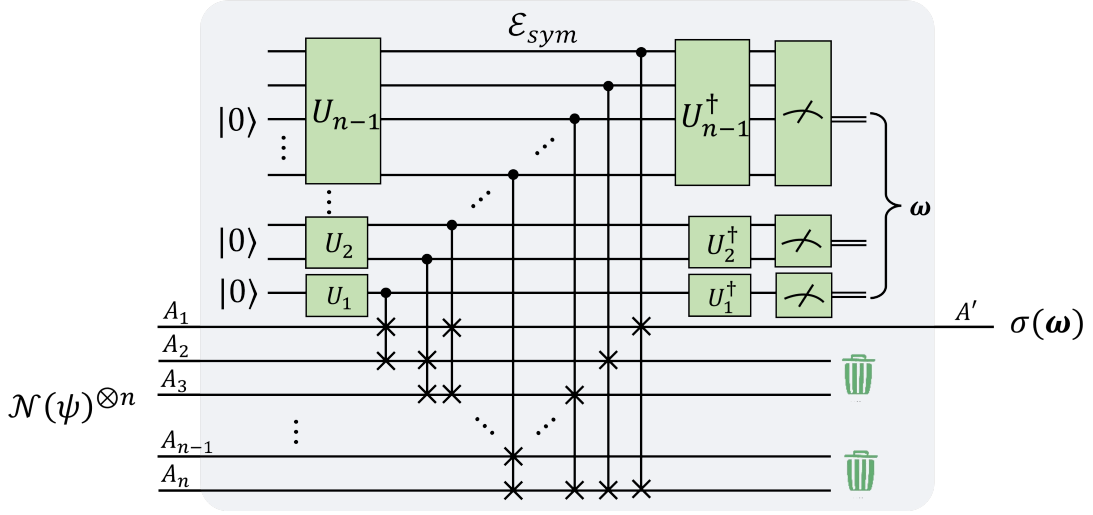


FIG. 4. Quantum circuit project quantum state to its symmetry subspace

with $\lambda_1 > \lambda_k, \forall k \geq 2$, and $\sum_{i=1}^d \psi_i = 1$. The λ_i are the eigenvalues, and the ψ_i are the noisy terms, which are orthogonal to the ideal pure state ψ . The output purified state is given in Eq. (A.1). Note that $\mathcal{N}(\psi)^j, \forall j$ share the same eigenvectors. For convenience, we order the eigenvalues in a descending sequence, $\lambda_1 > \lambda_2 \geq \dots \geq \lambda_d$, then the eigenvalues of the output purified state $\sigma(0)$ are

$$\lambda'_i = \frac{\lambda_i + \lambda_i^2 + \dots + \lambda_i^n}{1 + \sum_{m=1}^d \lambda_m^2 + \dots + \sum_{m=1}^d \lambda_m^n}. \quad (\text{A.3})$$

In particular,

$$\lambda'_1 - \lambda_1 = \frac{\lambda_1 + \lambda_1^2 + \dots + \lambda_1^n}{1 + \sum_{m=1}^d \lambda_m^2 + \dots + \sum_{m=1}^d \lambda_m^n} - \lambda_1 \quad (\text{A.4})$$

$$= \frac{\lambda_1^2 + \lambda_1^3 + \dots + \lambda_1^n - \lambda_1 \sum_{m=1}^d \lambda_m^2 - \dots - \lambda_1 \sum_{m=1}^d \lambda_m^n}{1 + \sum_{m=1}^d \lambda_m^2 + \dots + \sum_{m=1}^d \lambda_m^n} \quad (\text{A.5})$$

$$= \frac{\lambda_1^2 \sum_{m=1}^d \lambda_m - \lambda_1 \sum_{m=1}^d \lambda_m^2 + \dots + \lambda_1^n \sum_{m=1}^d \lambda_m - \lambda_1 \sum_{m=1}^d \lambda_m^n}{1 + \sum_{m=1}^d \lambda_m^2 + \dots + \sum_{m=1}^d \lambda_m^n} \quad (\text{A.6})$$

$$= \lambda_1 \frac{\sum_{m=1}^d \lambda_m (\lambda_1 - \lambda_m) + \dots + \lambda_m (\lambda_1^{n-1} - \lambda_m^{n-1})}{1 + \sum_{m=1}^d \lambda_m^2 + \dots + \sum_{m=1}^d \lambda_m^n} \quad (\text{A.7})$$

$$\geq 0. \quad (\text{A.8})$$

The equality holds when the noisy state is pure, i.e., no noise at all. Thus, for any input state ψ , the purified state has higher fidelity, i.e., $\lambda'_1 = F(\psi, \mathcal{E}(\mathcal{N}(\psi)^{\otimes 2})) \geq F(\psi, \mathcal{N}(\psi)) = \lambda_1$, which satisfies the definition of purification protocol. Here, we complete the proof. ■

When we take $n = 2$, then the symmetric projection reduces to the *swap test gadget* [37] as shown in FIG. 5. Since the swap test gadget is a special case of the symmetric projection, we directly have Swap test gadget is a $2 \rightarrow 1$ purification protocol for the set that contains all pure states.

Supplemental Material B: Formal definitions of average purification fidelity and optimal distributed purification protocol

To fairly compare the purification protocols, we define the *average purification fidelity* to quantify the performance of different purification protocols. The average purification fidelity only takes the successful cases into account. Specifically, sample quantum states from the state set uniformly, apply the purification protocol, rule out all the failure cases, and the average fidelity of the successful cases can be computed by $\bar{F}(n; \mathcal{S}, \mathcal{N}, \mathcal{E}) = \sum_{\psi \in \mathcal{S}} \frac{P_\psi}{\sum_{\psi \in \mathcal{S}} P_\psi} F(\sigma_\psi, \psi)$. Dividing $|\mathcal{S}|$ from the numerator and

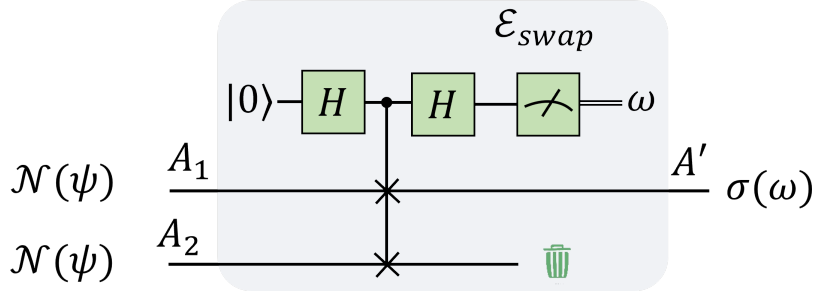


FIG. 5. Quantum circuit for $2 \rightarrow 1$ swap test gadget on arbitrary input noisy states $\mathcal{N}(\psi)$. The shaded area is the purification protocol $\mathcal{E}_{\text{swap}}$. The three-qubit gate between Hadamard gates is a controlled swap.

denominator, respectively, we arrive at $\bar{F}(n; \mathcal{S}, \mathcal{N}, \mathcal{E}) = \frac{1}{|\mathcal{S}|} \sum_{\psi \in \mathcal{S}} \frac{p_\psi}{\bar{P}} F(\sigma_\psi, \psi)$. Since the output state is $\psi = \frac{\tilde{\sigma}_\psi}{p_\psi}$, we have $\bar{F}(n; \mathcal{S}, \mathcal{N}, \mathcal{E}) = \frac{1}{|\mathcal{S}|} \sum_{\psi \in \mathcal{S}} F\left(\psi, \frac{\tilde{\sigma}_\psi}{\bar{P}}\right)$. Formally, the average purification fidelity is defined in the following.

Definition 2 (Average purification fidelity) For a given pure state set \mathcal{S} , noise channel \mathcal{N} and the $n \rightarrow 1$ distributed purification protocol \mathcal{E} , the average purification fidelity is defined as

$$\bar{F}(n; \mathcal{S}, \mathcal{N}, \mathcal{E}) = \frac{1}{|\mathcal{S}|} \sum_{\psi \in \mathcal{S}} F\left(\psi, \frac{\tilde{\sigma}_\psi}{\bar{P}}\right), \quad (\text{B.1})$$

where $\tilde{\sigma}_\psi$ is the unnormalized purified state.

Clearly, the performance of purification protocol depends on the average successful probability \bar{P} , which was also discussed in Ref. [34]. Thus, with a given average success probability \bar{P} , we define the *optimal purification protocol* as a protocol that achieves *optimal average purification fidelity* \bar{F}^* . Since this work focuses on the distributed purification protocol, we have to constrain the operation to LOCC. The *optimal distributed purification protocol* can be defined formally in the following.

Definition 3 (Optimal distributed purification protocol) For a given pure state set \mathcal{S} , noise channel \mathcal{N} and the average success probability \bar{P} , the optimal $n \rightarrow 1$ distributed purification protocol \mathcal{E}^* is a protocol that achieves the optimal average purification fidelity:

$$\begin{aligned} \bar{F}_{\text{LOCC}}^*(n, \bar{P}; \mathcal{S}, \mathcal{N}) &= \bar{F}(n; \mathcal{S}, \mathcal{N}, \mathcal{E}^*) \\ &= \max_{\mathcal{E}} \left\{ \bar{F}(n; \mathcal{S}, \mathcal{N}, \mathcal{E}) \mid \mathcal{E} \in \text{LOCC} \cap \text{CPTN}, \frac{1}{|\mathcal{S}|} \sum_{\psi \in \mathcal{S}} \text{Tr}[\mathcal{E}(\mathcal{N}(\psi)^{\otimes n})] = \bar{P} \right\}. \end{aligned} \quad (\text{B.2})$$

Supplemental Material C: Proof of Theorem 1

Theorem 1 (No-go theorem for the pure state set) For the two-qubit depolarizing noise channel \mathcal{N}_{AB}^γ with noise level $\gamma \in (0, 1)$, there is no non-trivial $2 \rightarrow 1$ LOCC purification protocol for the set that contains all pure states \mathcal{S}_P .

Proof At the beginning, we denote μ_P as the Haar measure of set \mathcal{S}_P ,

$$M_\psi = \mathcal{N}^{\otimes n}(\psi^{\otimes n})_{A^n B^n}^T \otimes (\psi - \text{Tr}[\psi \mathcal{N}(\psi)]I)_{A' B'} \text{ for any } \psi \in \mathcal{S}_P, \quad (\text{C.1})$$

$M = \mathbb{E}_{\psi \sim \mu_P} M_\psi$ as the expectation of M_ψ with respect to the Haar measure, and have that

$$\text{Tr}[J_{\mathcal{E}_{A^n B^n A' B'}} M] = \mathbb{E}_{\psi \sim \mu_P} \text{Tr}[J_{\mathcal{E}_{A^n B^n A' B'}}^T \mathcal{N}^{\otimes n} \otimes \mathcal{I}(\psi^{\otimes n+1})] - \text{Tr}[\psi \mathcal{N}(\psi)] \text{Tr}[J_{\mathcal{E}_{A^n B^n A' B'}}^T \mathcal{N}^{\otimes n}(\psi^{\otimes n}) \otimes I_{A' B'}]. \quad (\text{C.2})$$

Suppose that there exists a nontrivial $2 \rightarrow 1$ LOCC purification protocol, which is equivalent to having a feasible solution

$J_{\mathcal{E}_{A^n B^n A' B'}}$ such that the following constraints are satisfied:

$$\begin{cases} J_{\mathcal{E}_{A^n B^n A' B'}} \geq 0, \\ \text{Tr}_{A' B'} [J_{\mathcal{E}_{A^n B^n A' B'}}] \leq I_{A^n B^n}, \\ J_{\mathcal{E}_{A^n B^n A' B'}}^{T_{A^n A'}} \geq 0, \\ \forall \psi \in \mathcal{S}_P, \text{Tr}[J_{\mathcal{E}_{A^n B^n A' B'}} M_\psi] \geq 0, \\ \text{Tr}[J_{\mathcal{E}_{A^n B^n A' B'}} M] > 0. \end{cases} \quad (\text{C.3})$$

Note that for any $W = U \otimes V \in \text{SU}(2)^{\otimes 2}$, we have

$$M_{W\psi W^\dagger} = (\mathcal{N}^{\otimes n} (W\psi W^\dagger)^{\otimes n})_{A^n B^n}^T \otimes (W\psi W^\dagger - \text{Tr}[W\psi W^\dagger \mathcal{N}(W\psi W^\dagger)] I)_{A' B'} \quad (\text{C.4})$$

$$= (W_{A^n B^n}^{*\otimes n} \otimes W_{A' B'}) ((\mathcal{N}^{\otimes n} (\psi)^{\otimes n})_{A^n B^n}^T \otimes (\psi - \text{Tr}[\psi \mathcal{N}(\psi)] I)_{A' B'}) (W_{A^n B^n}^{T\otimes n} \otimes W_{A' B'}^\dagger) \quad (\text{C.5})$$

$$= (W_{A^n B^n}^{*\otimes n} \otimes W_{A' B'}) M_\psi (W_{A^n B^n}^{T\otimes n} \otimes W_{A' B'}^\dagger), \quad (\text{C.6})$$

$$\text{Tr}[J_{\mathcal{E}_{A^n B^n A' B'}} M] = \mathbb{E}_{\psi \sim \mu_P} \text{Tr}[J_{\mathcal{E}_{A^n B^n A' B'}} M_{W^\dagger \psi W}] \quad (\text{C.7})$$

$$= \mathbb{E}_{\psi \sim \mu_P} \text{Tr}[(W_{A^n B^n}^{*\otimes n} \otimes W_{A' B'}) J_{\mathcal{E}_{A^n B^n A' B'}} (W_{A^n B^n}^{T\otimes n} \otimes W_{A' B'}^\dagger) M_\psi] \quad (\text{C.8})$$

$$= \text{Tr}[(W_{A^n B^n}^{*\otimes n} \otimes W_{A' B'}) J_{\mathcal{E}_{A^n B^n A' B'}} (W_{A^n B^n}^{T\otimes n} \otimes W_{A' B'}^\dagger) M]. \quad (\text{C.9})$$

Moreover, since

$$J_{\mathcal{E}'_{A^n B^n A' B'}} := (W_{A^n B^n}^{*\otimes n} \otimes W_{A' B'}) J_{\mathcal{E}_{A^n B^n A' B'}} (W_{A^n B^n}^{T\otimes n} \otimes W_{A' B'}^\dagger) \quad (\text{C.10})$$

satisfies

$$\begin{cases} \text{Spec}(J_{\mathcal{E}'_{A^n B^n A' B'}}) = \text{Spec}(J_{\mathcal{E}_{A^n B^n A' B'}}), \\ \text{Tr}_{A' B'} [J_{\mathcal{E}'_{A^n B^n A' B'}}] = W_{A^n B^n}^{*\otimes n} \text{Tr}_{A' B'} [J_{\mathcal{E}_{A^n B^n A' B'}}] W_{A^n B^n}^{T\otimes n} \leq W_{A^n B^n}^{*\otimes n} I_{A^n B^n} W_{A^n B^n}^{T\otimes n} = I_{A^n B^n}, \\ \text{Spec}(J_{\mathcal{E}'_{A^n B^n A' B'}}^{T_{A^n A'}}) = \text{Spec}\left((U_{A^n}^{*\otimes n} \otimes U_{A'} \otimes V_{B^n}^{*\otimes n} \otimes V_{B'}) J_{\mathcal{E}_{A^n B^n A' B'}} (U_{A^n}^{T\otimes n} \otimes U_{A'}^\dagger \otimes V_{B^n}^{T\otimes n} \otimes V_{B'}^\dagger)\right)^{T_{A^n A'}}, \\ = \text{Spec}\left((U_{A^n}^{\otimes n} \otimes U_{A'}^* \otimes V_{B^n}^{\otimes n} \otimes V_{B'}) J_{\mathcal{E}_{A^n B^n A' B'}}^{T_{A^n A'}} (U_{A^n}^\dagger \otimes U_{A'}^T \otimes V_{B^n}^\dagger \otimes V_{B'}^T)\right) = \text{Spec}\left(J_{\mathcal{E}_{A^n B^n A' B'}}^{T_{A^n A'}}\right), \\ \forall \psi \in \mathcal{S}_P, \text{Tr}[J_{\mathcal{E}'_{A^n B^n A' B'}} M_\psi] = \text{Tr}[J_{\mathcal{E}_{A^n B^n A' B'}} M_{W^\dagger \psi W}] \geq 0, \\ \text{Tr}[J_{\mathcal{E}'_{A^n B^n A' B'}} M] = \text{Tr}[J_{\mathcal{E}_{A^n B^n A' B'}} M] > 0, \end{cases} \quad (\text{C.11})$$

we find that $J_{\mathcal{E}_{A^n B^n A' B'}}$ is a feasible solution to the constraints in Eq.(C.3) implies that $J_{\mathcal{E}'_{A^n B^n A' B'}}$ is also a feasible solution. Consider further, the linear combination of the feasible solutions is also feasible, i.e.,

$$J_{\bar{\mathcal{E}}_{A^n B^n A' B'}} = \mathbb{E}_{U, V \sim \mu_{\text{SU}(2)}} J_{\mathcal{E}'_{A^n B^n A' B'}} = \mathbb{E}_{W \sim \mu_{\text{SU}(2)^{\otimes 2}}} (W_{A^n B^n}^{*\otimes n} \otimes W_{A' B'}) J_{\mathcal{E}_{A^n B^n A' B'}} (W_{A^n B^n}^{T\otimes n} \otimes W_{A' B'}^\dagger), \quad (\text{C.12})$$

is also feasible. By the irreducible representation decomposition of

$$\text{SU}(2) \rightarrow \text{SU}(8) : U \mapsto U^{*\otimes 2} \otimes U = 2U \oplus f_4(U), \quad (\text{C.13})$$

we have

$$\exists G \in \text{SU}(8), \text{ s.t. } \forall U \in \text{SU}(2), G(U^{*\otimes 2} \otimes U)G^\dagger = \begin{pmatrix} I_2 \otimes U & \\ & f_4(U) \end{pmatrix}, \quad (\text{C.14})$$

where f_4 is a 4-dimensional irreducible representation of $\text{SU}(2)$. Moreover, by the irreducible representation decomposition of

$$\text{SU}(2)^{\otimes 2} \rightarrow \text{SU}(64) : U \otimes V \mapsto U^{*\otimes 2} \otimes V^{*\otimes 2} \otimes U \otimes V = 4U \otimes V \oplus 2U \otimes f_4(V) \oplus 2V \otimes f_4(U) \otimes f_4(U) \otimes f_4(V), \quad (\text{C.15})$$

we have $\exists \tilde{G} \in \text{SU}(64)$, s.t. $\forall U \otimes V \in \text{SU}(2)^{\otimes 2}$,

$$\tilde{G}(U^{*\otimes 2} \otimes V^{*\otimes 2} \otimes U \otimes V)\tilde{G}^\dagger = \begin{pmatrix} I_4 \otimes U \otimes V & & & \\ & I_2 \otimes U \otimes f_4(V) & & \\ & & I_2 \otimes V \otimes f_4(U) & \\ & & & f_4(U) \otimes f_4(V) \end{pmatrix}, \quad (\text{C.16})$$

where f_4 is a 4-dimensional irreducible representation of $SU(2)$. The following computation is based on a specific \tilde{G} which could be found in Supplemental Material D. Otherwise, using other \tilde{G} may introduce basis transformations. Since $J_{\mathcal{E}_{A^n B^n A' B'}}$ is commutative with

$$U_{A^n}^{*\otimes n} \otimes V_{B^n}^{*\otimes n} \otimes U_{A'} \otimes V_{B'}, \text{ for any } U, V \in SU(2), \quad (\text{C.17})$$

by mixed Schur–Weyl duality[61], we have $\tilde{G} J_{\mathcal{E}_{A^n B^n A' B'}} \tilde{G}^\dagger$ is always of form

$$\tilde{G} J_{\mathcal{E}_{A^n B^n A' B'}} \tilde{G}^\dagger = \begin{pmatrix} H_0 \otimes I_4 & & & \\ & H_1 \otimes I_8 & & \\ & & H_2 \otimes I_8 & \\ & & & h_3 I_{16} \end{pmatrix} = \begin{pmatrix} H_0 & & & \\ & H_1 \otimes I_2 & & \\ & & H_2 \otimes I_2 & \\ & & & h_3 I_4 \end{pmatrix} \otimes I_4, \quad (\text{C.18})$$

where $H_0 \in \mathbb{C}^{4 \times 4}$, $H_1, H_2 \in \mathbb{C}^{2 \times 2}$, $h_3 \in \mathbb{C}$. Simultaneously, we find

$$\tilde{G} J_{\mathcal{E}_{A^n B^n A' B'}}^{T_B} \tilde{G}^\dagger = \begin{pmatrix} (I_2 \otimes Z) H_0^{T_B} (I_2 \otimes Z) & & & \\ & H_1 \otimes I_2 & & \\ & & Z H_2^T Z \otimes I_2 & \\ & & & h_3 I_4 \end{pmatrix} \otimes I_4, \quad (\text{C.19})$$

$$\text{Spec}(\text{Tr}_{A' B'} [J_{\mathcal{E}_{A^n B^n A' B'}}]) = \left\{ \frac{4}{9} \langle 00 | H_0 | 00 \rangle + \frac{8}{9} \langle 0 | H_1 | 0 \rangle + \frac{8}{9} \langle 0 | H_2 | 0 \rangle + \frac{16}{9} h_3, \right. \quad (\text{C.20})$$

$$\left. \frac{4}{3} \langle 01 | H_0 | 01 \rangle + \frac{8}{3} \langle 1 | H_2 | 1 \rangle, \frac{4}{3} \langle 10 | H_0 | 10 \rangle + \frac{8}{3} \langle 1 | H_1 | 1 \rangle, 4 \langle 11 | H_0 | 11 \rangle \right\}, \quad (\text{C.21})$$

where $\langle jk | H_0^{T_B} | lr \rangle = \langle jr | H_0 | lk \rangle$ for any $j, k, l, r = 0, 1$. Denote Tr_d as the partial trace on the last d -dimensional system, the block representations of $\text{Tr}_4[\tilde{G} M_\psi \tilde{G}^\dagger]$ and $\text{Tr}_4[\tilde{G} M \tilde{G}^\dagger]$ as

$$\text{Tr}_4[\tilde{G} M_\psi \tilde{G}^\dagger] = \sum_{j,k=0}^3 |j\rangle\langle k| \otimes M_\psi^{(jk)}, \quad \text{Tr}_4[\tilde{G} M \tilde{G}^\dagger] = \sum_{j,k=0}^3 |j\rangle\langle k| \otimes M^{(jk)}, \quad (\text{C.22})$$

and we have

$$\text{Tr}[J_{\mathcal{E}_{A^n B^n A' B'}} M] = \text{Tr}[H_0 M^{(00)}] + \text{Tr}[H_1 \text{Tr}_2[M^{(11)}]] + \text{Tr}[H_2 \text{Tr}_2[M^{(22)}]] + h_3 \text{Tr}[M^{(33)}]. \quad (\text{C.23})$$

Then we obtain an SDP related to the constraints (C.3)

$$\max \text{Tr}[H_0 M^{(00)}] + \text{Tr}[H_1 \text{Tr}_2[M^{(11)}]] + \text{Tr}[H_2 \text{Tr}_2[M^{(22)}]] + h_3 \text{Tr}[M^{(33)}] \quad (\text{C.24a})$$

$$\text{s.t. } H_0, H_1, H_2, h_3, H_0^{T_B} \geq 0; \quad (\text{C.24b})$$

$$\frac{4}{9} \langle 00 | H_0 | 00 \rangle + \frac{8}{9} \langle 0 | H_1 | 0 \rangle + \frac{8}{9} \langle 0 | H_2 | 0 \rangle + \frac{16}{9} h_3 \leq 1; \quad (\text{C.24c})$$

$$\frac{4}{3} \langle 10 | H_0 | 10 \rangle + \frac{8}{3} \langle 1 | H_1 | 1 \rangle \leq 1; \quad (\text{C.24d})$$

$$\frac{4}{3} \langle 01 | H_0 | 01 \rangle + \frac{8}{3} \langle 1 | H_2 | 1 \rangle \leq 1; \quad (\text{C.24e})$$

$$4 \langle 11 | H_0 | 11 \rangle \leq 1; \quad (\text{C.24f})$$

$$\forall \psi, \text{Tr}[H_0 M_\psi^{(00)}] + \text{Tr}[H_1 \text{Tr}_2[M_\psi^{(11)}]] + \text{Tr}[H_2 \text{Tr}_2[M_\psi^{(22)}]] + h_3 \text{Tr}[M_\psi^{(33)}] \geq 0. \quad (\text{C.24g})$$

and its relaxation

$$\max \text{Tr}[H_0 M^{(00)}] + \text{Tr}[H_1 \text{Tr}_2[M^{(11)}]] + \text{Tr}[H_2 \text{Tr}_2[M^{(22)}]] + h_3 \text{Tr}[M^{(33)}] \quad (\text{C.25a})$$

$$\text{s.t. } H_0, H_1, H_2, h_3, H_0^{T_B} \geq 0; \quad (\text{C.25b})$$

$$\frac{4}{9} \langle 00 | H_0 | 00 \rangle + \frac{8}{9} \langle 0 | H_1 | 0 \rangle + \frac{8}{9} \langle 0 | H_2 | 0 \rangle + \frac{16}{9} h_3 \leq 1; \quad (\text{C.25c})$$

$$\frac{4}{3} \langle 10 | H_0 | 10 \rangle + \frac{8}{3} \langle 1 | H_1 | 1 \rangle \leq 1; \quad (\text{C.25d})$$

$$\frac{4}{3}\langle 01|H_0|01\rangle + \frac{8}{3}\langle 1|H_2|1\rangle \leq 1; \quad (\text{C.25e})$$

$$4\langle 11|H_0|11\rangle \leq 1; \quad (\text{C.25f})$$

$$\text{Tr}[H_0 M_{|\Phi\rangle+}^{(00)}] + \text{Tr}[H_1 \text{Tr}_2[M_{|\Phi\rangle+}^{(11)}]] + \text{Tr}[H_2 \text{Tr}_2[M_{|\Phi\rangle+}^{(22)}]] + h_3 \text{Tr}[M_{|\Phi\rangle+}^{(33)}] \geq 0. \quad (\text{C.25g})$$

It is checked that for any $\gamma \in [0, 1]$,

$$\text{Tr}_2[M^{(11)}] = \text{Tr}_2[M^{(22)}] = \text{Diag}\left(-\frac{1}{120}(1-\gamma)(27\gamma^2 - 56\gamma + 80), -\frac{1}{40}\gamma(1-\gamma)(32 - 15\gamma)\right) \leq 0, \quad (\text{C.26})$$

$$\text{Tr}[M^{(33)}] = -\frac{1}{60}(1-\gamma)(27\gamma^2 - 56\gamma + 80) \leq 0, \quad (\text{C.27})$$

$$\text{Tr}_2[M_{|\Phi\rangle+}^{(11)}] = \text{Tr}_2[M_{|\Phi\rangle+}^{(22)}] = \text{Diag}\left(-\frac{1}{24}(1-\gamma)(3\gamma^2 - 6\gamma + 16), -\frac{3}{8}\gamma(1-\gamma)(2-\gamma)\right) \leq 0, \quad (\text{C.28})$$

$$\text{Tr}[M_{|\Phi\rangle+}^{(33)}] = -\frac{1}{12}(1-\gamma)(3\gamma^2 - 6\gamma + 10) \leq 0. \quad (\text{C.29})$$

Hence for any optimal solution $(H_0, H_1, H_2, h_3) = (\check{H}_0, \check{H}_1, \check{H}_2, \check{h}_3)$ of SDP (C.25), $(H_0, H_1, H_2, h_3) = (\check{H}_0, 0, 0, 0)$ must also be a feasible solution because for any $\gamma \in [0, 1]$

$$\frac{4}{9}\langle 00|\check{H}_0|00\rangle \leq \frac{4}{9}\langle 00|\check{H}_0|00\rangle + \frac{8}{9}\langle 0|\check{H}_1|0\rangle + \frac{8}{9}\langle 0|\check{H}_2|0\rangle + \frac{16}{9}\check{h}_3 \leq 1, \quad (\text{C.30})$$

$$\frac{4}{3}\langle 10|\check{H}_0|10\rangle \leq \frac{4}{3}\langle 10|\check{H}_0|10\rangle + \frac{8}{3}\langle 1|\check{H}_1|1\rangle \leq 1, \quad (\text{C.31})$$

$$\frac{4}{3}\langle 01|\check{H}_0|01\rangle \leq \frac{4}{3}\langle 01|\check{H}_0|01\rangle + \frac{8}{3}\langle 1|\check{H}_2|1\rangle \leq 1, \quad (\text{C.32})$$

$$\text{Tr}[\check{H}_0 M_{|\Phi\rangle+}^{(00)}] \geq \text{Tr}[\check{H}_0 M_{|\Phi\rangle+}^{(00)}] + \text{Tr}[\check{H}_1 \text{Tr}_2[M_{|\Phi\rangle+}^{(11)}]] + \text{Tr}[\check{H}_2 \text{Tr}_2[M_{|\Phi\rangle+}^{(22)}]] + \check{h}_3 \text{Tr}[M_{|\Phi\rangle+}^{(33)}] \geq 0. \quad (\text{C.33})$$

Moreover, for any $\gamma \in [0, 1]$, by

$$\text{Tr}[\check{H}_0 M^{(00)}] + \text{Tr}[\check{H}_1 \text{Tr}_2[M^{(11)}]] + \text{Tr}[\check{H}_2 \text{Tr}_2[M^{(22)}]] + \check{h}_3 \text{Tr}[M^{(33)}] \leq \text{Tr}[\check{H}_0 M^{(00)}] \quad (\text{C.34})$$

$(H_0, H_1, H_2, h_3) = (\check{H}_0, 0, 0, 0)$ is also an optimal solution of SDP (C.25). Therefore, we could let $H_1 = H_2 = h_3 = 0$, or equivalently

$$J_{\mathcal{E}_{A^n B^n A' B'}} = \check{G}(|00\rangle\langle 00| \otimes H_0 \otimes I_4) \check{G}^\dagger, \quad (\text{C.35})$$

and find the following SDP has equivalent maximum with (C.25).

$$\max \text{Tr}[H_0 M^{(00)}] \quad (\text{C.36a})$$

$$\text{s.t. } H_0, H_0^{TB} \geq 0; \quad (\text{C.36b})$$

$$\langle 00|H_0|00\rangle \leq \frac{9}{4}, \quad \langle 11|H_0|11\rangle \leq \frac{1}{4}; \quad (\text{C.36c})$$

$$\langle 10|H_0|10\rangle \leq \frac{3}{4}, \quad \langle 01|H_0|01\rangle \leq \frac{3}{4}; \quad (\text{C.36d})$$

$$\text{Tr}[H_0 M_{|\Phi\rangle+}^{(00)}] \geq 0. \quad (\text{C.36e})$$

where

$$VM^{(00)}V^\dagger = -(1-\gamma) \text{Diag}\left(\frac{1}{16}\gamma(4-3\gamma), -\frac{3}{80}\gamma(4-3\gamma), \frac{1}{80}\gamma(32-15\gamma), \frac{1}{240}(27\gamma^2 - 56\gamma + 80)\right), \quad (\text{C.37})$$

$$VM_{|\Phi\rangle+}^{(00)}V^\dagger = -(1-\gamma) \begin{pmatrix} \frac{1}{16}\gamma(4-3\gamma) & 0 & 0 & 0 \\ 0 & -\frac{3}{80}\gamma(4-3\gamma) & 0 & -\frac{1}{20}\gamma(4-3\gamma) \\ 0 & 0 & \frac{1}{16}\gamma(8-3\gamma) & 0 \\ 0 & -\frac{1}{20}\gamma(4-3\gamma) & 0 & \frac{1}{240}(123\gamma^2 - 264\gamma + 200) \end{pmatrix}, \quad (\text{C.38})$$

$$\text{for } V = \begin{pmatrix} 0 & \frac{1}{\sqrt{2}} & \frac{1}{\sqrt{2}} & 0 \\ -\frac{3}{\sqrt{10}} & 0 & 0 & \frac{1}{\sqrt{10}} \\ 0 & -\frac{1}{\sqrt{2}} & \frac{1}{\sqrt{2}} & 0 \\ \frac{1}{\sqrt{10}} & 0 & 0 & \frac{3}{\sqrt{10}} \end{pmatrix}. \quad (\text{C.39})$$

Denote the set of d -dimensional positive semi-definite Hermitian as \mathcal{L}_d^+ . By Peres–Horodecki criterion [62, 63], the 4-dimensional Hermitian H_0 satisfies $H_0 \geq 0$ and $H_0^{TB} \geq 0$ if and only if H_0 is separable, i.e. there exist several $H_{0j}^A, H_{0j}^B \in \mathcal{L}_2^+$ with $H_0 = \sum_j H_{0j}^A \otimes H_{0j}^B$. Thus we have an equivalent programming with (C.36):

$$\max \operatorname{Tr}[(\sum_j H_{0j}^A \otimes H_{0j}^B)M^{(00)}] \quad (\text{C.40a})$$

$$\text{s.t. } \forall j, H_{0j}^A, H_{0j}^B \in \mathcal{L}_2^+; \quad (\text{C.40b})$$

$$\langle 00 | (\sum_j H_{0j}^A \otimes H_{0j}^B) | 00 \rangle \leq \frac{9}{4}, \quad \langle 11 | (\sum_j H_{0j}^A \otimes H_{0j}^B) | 11 \rangle \leq \frac{1}{4}; \quad (\text{C.40c})$$

$$\langle 10 | (\sum_j H_{0j}^A \otimes H_{0j}^B) | 10 \rangle \leq \frac{3}{4}, \quad \langle 01 | (\sum_j H_{0j}^A \otimes H_{0j}^B) | 01 \rangle \leq \frac{3}{4}; \quad (\text{C.40d})$$

$$\operatorname{Tr}[(\sum_j H_{0j}^A \otimes H_{0j}^B)M_{|\Phi\rangle^+}^{(00)}] \geq 0. \quad (\text{C.40e})$$

We claim that

$$H_0^A, H_0^B \in \mathcal{L}_2^+, \gamma \in (0, 1) \implies \operatorname{Tr}[(H_0^A \otimes H_0^B)M_{|\Phi\rangle^+}^{(00)}] \leq 0, \quad (\text{C.41})$$

$$H_0^A, H_0^B \in \mathcal{L}_2^+, \gamma \in (0, 1), \operatorname{Tr}[(H_0^A \otimes H_0^B)M_{|\Phi\rangle^+}^{(00)}] = 0 \implies \operatorname{Tr}[(H_0^A \otimes H_0^B)M^{(00)}] \leq 0, \quad (\text{C.42})$$

which will be proved after this proof. By these two claims, we find 0 is an upper bound of the maximum of (C.40) because

$$\gamma \in (0, 1) \bigwedge (\forall j, H_{0j}^A, H_{0j}^B \in \mathcal{L}_2^+) \bigwedge \operatorname{Tr}[(\sum_j H_{0j}^A \otimes H_{0j}^B)M_{|\Phi\rangle^+}^{(00)}] \geq 0 \quad (\text{C.43})$$

$$\stackrel{\text{(C.41)}}{\implies} \gamma \in (0, 1) \bigwedge (\forall j, H_{0j}^A, H_{0j}^B \in \mathcal{L}_2^+, \operatorname{Tr}[(H_{0j}^A \otimes H_{0j}^B)M_{|\Phi\rangle^+}^{(00)}] \leq 0) \bigwedge \operatorname{Tr}[(\sum_j H_{0j}^A \otimes H_{0j}^B)M_{|\Phi\rangle^+}^{(00)}] \geq 0 \quad (\text{C.44})$$

$$\iff \gamma \in (0, 1) \bigwedge (\forall j, H_{0j}^A, H_{0j}^B \in \mathcal{L}_2^+, \operatorname{Tr}[(H_{0j}^A \otimes H_{0j}^B)M_{|\Phi\rangle^+}^{(00)}] = 0) \quad (\text{C.45})$$

$$\stackrel{\text{(C.42)}}{\implies} \forall j, \operatorname{Tr}[(H_{0j}^A \otimes H_{0j}^B)M^{(00)}] \leq 0 \quad (\text{C.46})$$

$$\implies \operatorname{Tr}[(\sum_j H_{0j}^A \otimes H_{0j}^B)M^{(00)}] \leq 0. \quad (\text{C.47})$$

On the other hand, feasible solution with each $H_{0j}^A = H_{0j}^B = 0$ suggests 0 is also an lower bound of the maximum of (C.40). As a result, the maximal values of programming (C.40) and SDPs (C.36) and (C.25) are all 0, and the maximal value of (C.24) is at most 0, which implies that (C.3) has no feasible solution. ■

Proof of (C.41). Claim (C.41) could be considered as a corollary of following Theorem 2, which is proved independent of this section. Here we could give another proof based on symbolic computation automatic reasoning using the cylindrical algebraic decomposition algorithm [64–67]. After setting

$$H_0^A = \begin{pmatrix} a & b + id \\ b - id & c \end{pmatrix}, \quad H_0^B = \begin{pmatrix} e & f + ih \\ f - ih & g \end{pmatrix}, \quad (\text{C.48})$$

with real variables $\{a, b, c, d, e, f, g, h\}$, we could use a system of inequalities

$$\{a \geq 0, c \geq 0, ac \geq b^2 + d^2, e \geq 0, g \geq 0, eg \geq f^2 + h^2\} \quad (\text{C.49})$$

to indicate $H_0^A, H_0^B \geq 0$ equivalently. Now we introduce another system of inequalities

$$\{a \geq 0, c \geq 0, ac \geq b^2 + d^2, e \geq 0, g \geq 0, eg \geq f^2 + h^2, 0 < \gamma < 1, \\ (-3\gamma^2 + 6\gamma - 4)ae + 9\gamma(\gamma - 2)(ag + ce) - 9(3\gamma^2 - 6\gamma + 4)cg + 24(\gamma - 1)bf + 24dh > 0\} \quad (\text{C.50})$$

where the left hand of the last inequality equals to $48 \operatorname{Tr}[(H_0^A \otimes H_0^B)M_{|\Phi\rangle^+}^{(00)}]/(1 - \gamma)$ because

$$48M_{|\Phi\rangle^+}^{(00)}/(1 - \gamma) = \begin{pmatrix} -3\gamma^2 + 6\gamma - 4 & 0 & 0 & 6(\gamma - 2) \\ 0 & 9(\gamma - 2)\gamma & 6\gamma & 0 \\ 0 & 6\gamma & 9(\gamma - 2)\gamma & 0 \\ 6(\gamma - 2) & 0 & 0 & -9(3\gamma^2 - 6\gamma + 4) \end{pmatrix}. \quad (\text{C.51})$$

Thus the semialgebraic set defined by (C.50) is exactly the feasible solutions of constraints

$$H_0^A, H_0^B \in \mathcal{L}_2^+, \gamma \in (0, 1), \text{Tr}[(H_0^A \otimes H_0^B)M_{|\Phi\rangle^+}^{(00)}] > 0. \quad (\text{C.52})$$

However, when we use the cylindrical algebraic decomposition algorithm [64–67] on (C.50), we will always obtain **False**, which derives that claim (C.41) always holds. ■

Proof of (C.42). Analogous to the proof of Claim (C.41), Claim (C.42) could also be proved by the cylindrical algebraic decomposition algorithm from symbolic computation automatic reasoning. To prove Claim (C.42), it is equivalent to prove the following constrains

$$\begin{cases} \gamma \in (0, 1), \\ H_0^A, H_0^B \in \mathcal{L}_2^+, \\ \text{Tr}[(H_0^A \otimes H_0^B)M_{|\Phi\rangle^+}^{(00)}]/(1-\gamma) = 0, \\ \text{Tr}[(H_0^A \otimes H_0^B)M^{(00)}]/(1-\gamma) > 0, \end{cases} \quad (\text{C.53})$$

are not feasible. After setting

$$H_0^A = \begin{pmatrix} a & b+id \\ b-id & c \end{pmatrix}, H_0^B = \begin{pmatrix} e & f+ih \\ f-ih & g \end{pmatrix}, \quad (\text{C.54})$$

with real variables $\{a, b, c, d, e, f, g, h\}$, we have established a system of inequalities equivalent to constrains (C.53):

$$\begin{cases} \{a \geq 0, c \geq 0, ac \geq b^2 + d^2, e \geq 0, g \geq 0, eg \geq f^2 + h^2, 0 < \gamma < 1, \\ (-3\gamma^2 + 6\gamma - 4)ae + 9\gamma(\gamma - 2)(ag + ce) - 9(3\gamma^2 - 6\gamma + 4)cg + 24(\gamma - 1)bf + 24dh = 0, \\ (-27\gamma^2 + 38\gamma - 8)ae + 3\gamma(15\gamma - 26)(ag + ce) - 9(3\gamma^2 - 6\gamma + 8)cg + 48(\gamma - 1)bf + 24(\gamma + 2)dh > 0\} \end{cases} \quad (\text{C.55})$$

where the left hand of the last inequality equals to $240 \text{Tr}[(H_0^A \otimes H_0^B)M^{(00)}]/(1-\gamma)$ because

$$240M^{(00)}/(1-\gamma) = \begin{pmatrix} -27\gamma^2 + 38\gamma - 8 & 0 & 0 & 6(\gamma - 4) \\ 0 & 3\gamma(15\gamma - 26) & 18\gamma & 0 \\ 0 & 18\gamma & 3\gamma(15\gamma - 26) & 0 \\ 6(\gamma - 4) & 0 & 0 & -9(3\gamma^2 - 6\gamma + 8) \end{pmatrix}. \quad (\text{C.56})$$

When we use the cylindrical algebraic decomposition algorithm [64–67] on (C.55), we will always obtain **False**, which derives that claim (C.42) always holds. The time cost of the cylindrical algebraic decomposition algorithm depends on the order of the variables. The time cost would be 2.5 seconds with order $(\gamma, a, e, c, g, b, d, f, h)$, but 8.5 hours with order $(\gamma, a, b, c, d, e, f, g, h)$ when we use the ‘‘CylindricalDecomposition’’ function [68] (or ‘‘Reduce’’ function [69]) in Wolfram Mathematica [70] on a workstation equipped with an Intel Core i9-14900K CPU and 48 GB RAM (2×24 GB, 8000 MT/s). ■

By Schmidt decomposition [38], any pure state of dimension 4 could be rewritten as $|\psi\rangle = \sigma_0|\psi_0^A\rangle|\psi_0^B\rangle + \sigma_1|\psi_1^A\rangle|\psi_1^B\rangle$ with $\sigma_0, \sigma_1 \geq 0$, $\langle\psi_j^A|\psi_k^A\rangle = \langle\psi_j^B|\psi_k^B\rangle = \delta_{jk}$ which is Kronecker delta. Denote

$$q = \sigma_0^2\sigma_1^2 \in [0, \frac{1}{4}], \quad (\text{C.57})$$

and we have all of $M_{|\psi\rangle}^{(00)}, \text{Tr}_2[M_{|\psi\rangle}^{(11)}], \text{Tr}_2[M_{|\psi\rangle}^{(22)}], \text{Tr}[M_{|\psi\rangle}^{(33)}]$ only depend on γ and q , and moreover linear on q :

$$VM_{|\psi\rangle}^{(00)}V^\dagger = \frac{1-\gamma}{720} \begin{pmatrix} 45\gamma(3\gamma-4) & 0 & 0 & 0 \\ 0 & 27\gamma(4-3\gamma) & 0 & 24\gamma(4-3\gamma)(10q-1) \\ 0 & 0 & 15\gamma(9\gamma-32q-16) & 0 \\ 0 & 24\gamma(4-3\gamma)(10q-1) & 0 & 111\gamma^2 - 248\gamma - 1920\gamma^2q + 4160\gamma q - 2400q \end{pmatrix} \quad (\text{C.58})$$

$$\text{Tr}_2[M_{|\psi\rangle}^{(11)}] = \text{Tr}_2[M_{|\psi\rangle}^{(22)}] = \frac{1-\gamma}{72} \text{Diag}(-21\gamma^2 + 44\gamma + 48\gamma^2q - 104\gamma q - 48, 3\gamma(9\gamma + 8q - 20)) \quad (\text{C.59})$$

$$\text{Tr}[M_{|\psi\rangle}^{(33)}] = \frac{1-\gamma}{36} (-21\gamma^2 + 44\gamma + 48\gamma^2q - 104\gamma q + 120q - 60), \quad (\text{C.60})$$

Furthermore, it is checked that $\text{Tr}_2[M_{|\psi\rangle}^{(11)}], \text{Tr}_2[M_{|\psi\rangle}^{(22)}]$ are both negative semi-definite, and $\text{Tr}[M_{|\psi\rangle}^{(33)}]$ is always non-positive for $\gamma \in (0, 1)$ and $q \in [0, \frac{1}{4}]$. Especially, we find that

$$q = \frac{1}{10} \implies (M_{|\psi\rangle}^{(00)}, \text{Tr}_2[M_{|\psi\rangle}^{(11)}], \text{Tr}_2[M_{|\psi\rangle}^{(22)}], \text{Tr}[M_{|\psi\rangle}^{(33)}]) = (M^{(00)}, \text{Tr}_2[M^{(11)}], \text{Tr}_2[M^{(22)}], \text{Tr}[M^{(33)}]), \quad (\text{C.61})$$

which indicates that the maximum point of $\text{Tr}[H_0 M^{(00)}]$ is the same as the maximum point of $\text{Tr}[H_0 M_{|\psi\rangle}^{(00)}]$ for any pure state $|\psi\rangle$, which implies that

Corollary 7 (No-go theorem for the maximally entangled state set) *For the two-qubit depolarizing noise channel \mathcal{N}_{AB}^γ with noise level γ , there is no non-trivial $2 \rightarrow 1$ LOCC purification protocol for any set containing all maximally entangled pure states.*

Supplemental Material D: The specific \tilde{G} in Supplemental Material C

The matrix \tilde{G} is a sparse matrix, and all the non-zero elements are shown as follows:

$$\begin{aligned}
& \{1, 13\} \rightarrow \frac{1}{6}, \{1, 25\} \rightarrow \frac{1}{6}, \{1, 30\} \rightarrow \frac{1}{3}, \{1, 37\} \rightarrow \frac{1}{6}, \{1, 47\} \rightarrow \frac{1}{3}, \{1, 49\} \rightarrow \frac{1}{6}, \{1, 54\} \rightarrow \frac{1}{3}, \{1, 59\} \rightarrow \frac{1}{3}, \{1, 64\} \rightarrow \frac{2}{3}, \\
& \{2, 9\} \rightarrow -\frac{1}{3}, \{2, 14\} \rightarrow -\frac{1}{6}, \{2, 26\} \rightarrow -\frac{1}{6}, \{2, 33\} \rightarrow -\frac{1}{3}, \{2, 38\} \rightarrow -\frac{1}{6}, \{2, 43\} \rightarrow -\frac{2}{3}, \{2, 48\} \rightarrow -\frac{1}{3}, \{2, 50\} \rightarrow -\frac{1}{6}, \\
& \{2, 60\} \rightarrow -\frac{1}{3}, \{3, 5\} \rightarrow -\frac{1}{3}, \{3, 15\} \rightarrow -\frac{1}{6}, \{3, 17\} \rightarrow -\frac{1}{3}, \{3, 22\} \rightarrow -\frac{2}{3}, \{3, 27\} \rightarrow -\frac{1}{6}, \{3, 32\} \rightarrow -\frac{1}{3}, \{3, 39\} \rightarrow -\frac{1}{6}, \\
& \{3, 51\} \rightarrow -\frac{1}{6}, \{3, 56\} \rightarrow -\frac{1}{3}, \{4, 1\} \rightarrow \frac{2}{3}, \{4, 6\} \rightarrow \frac{1}{3}, \{4, 11\} \rightarrow \frac{1}{3}, \{4, 16\} \rightarrow \frac{1}{6}, \{4, 18\} \rightarrow \frac{1}{3}, \{4, 28\} \rightarrow \frac{1}{6}, \{4, 35\} \rightarrow \frac{1}{3}, \\
& \{4, 40\} \rightarrow \frac{1}{6}, \{4, 52\} \rightarrow \frac{1}{6}, \{5, 13\} \rightarrow \frac{i}{2\sqrt{3}}, \{5, 25\} \rightarrow -\frac{i}{2\sqrt{3}}, \{5, 37\} \rightarrow \frac{i}{2\sqrt{3}}, \{5, 47\} \rightarrow \frac{i}{\sqrt{3}}, \{5, 49\} \rightarrow -\frac{i}{2\sqrt{3}}, \\
& \{5, 59\} \rightarrow -\frac{i}{\sqrt{3}}, \{6, 14\} \rightarrow \frac{i}{2\sqrt{3}}, \{6, 26\} \rightarrow -\frac{i}{2\sqrt{3}}, \{6, 38\} \rightarrow \frac{i}{2\sqrt{3}}, \{6, 48\} \rightarrow \frac{i}{\sqrt{3}}, \{6, 50\} \rightarrow -\frac{i}{2\sqrt{3}}, \{6, 60\} \rightarrow -\frac{i}{\sqrt{3}}, \\
& \{7, 5\} \rightarrow -\frac{i}{\sqrt{3}}, \{7, 15\} \rightarrow -\frac{i}{2\sqrt{3}}, \{7, 17\} \rightarrow \frac{i}{\sqrt{3}}, \{7, 27\} \rightarrow \frac{i}{2\sqrt{3}}, \{7, 39\} \rightarrow -\frac{i}{2\sqrt{3}}, \{7, 51\} \rightarrow \frac{i}{2\sqrt{3}}, \{8, 6\} \rightarrow -\frac{i}{\sqrt{3}}, \\
& \{8, 16\} \rightarrow -\frac{i}{2\sqrt{3}}, \{8, 18\} \rightarrow \frac{i}{\sqrt{3}}, \{8, 28\} \rightarrow \frac{i}{2\sqrt{3}}, \{8, 40\} \rightarrow -\frac{i}{2\sqrt{3}}, \{8, 52\} \rightarrow \frac{i}{2\sqrt{3}}, \{9, 13\} \rightarrow \frac{i}{2\sqrt{3}}, \{9, 25\} \rightarrow \frac{i}{2\sqrt{3}}, \\
& \{9, 30\} \rightarrow \frac{i}{\sqrt{3}}, \{9, 37\} \rightarrow -\frac{i}{2\sqrt{3}}, \{9, 49\} \rightarrow -\frac{i}{2\sqrt{3}}, \{9, 54\} \rightarrow -\frac{i}{\sqrt{3}}, \{10, 9\} \rightarrow -\frac{i}{\sqrt{3}}, \{10, 14\} \rightarrow -\frac{i}{2\sqrt{3}}, \{10, 26\} \rightarrow -\frac{i}{2\sqrt{3}}, \\
& \{10, 33\} \rightarrow \frac{i}{\sqrt{3}}, \{10, 38\} \rightarrow \frac{i}{2\sqrt{3}}, \{10, 50\} \rightarrow \frac{i}{2\sqrt{3}}, \{11, 15\} \rightarrow \frac{i}{2\sqrt{3}}, \{11, 27\} \rightarrow \frac{i}{2\sqrt{3}}, \{11, 32\} \rightarrow \frac{i}{\sqrt{3}}, \{11, 39\} \rightarrow -\frac{i}{2\sqrt{3}}, \\
& \{11, 51\} \rightarrow -\frac{i}{2\sqrt{3}}, \{11, 56\} \rightarrow -\frac{i}{\sqrt{3}}, \{12, 11\} \rightarrow -\frac{i}{\sqrt{3}}, \{12, 16\} \rightarrow -\frac{i}{2\sqrt{3}}, \{12, 28\} \rightarrow -\frac{i}{2\sqrt{3}}, \{12, 35\} \rightarrow \frac{i}{\sqrt{3}}, \\
& \{12, 40\} \rightarrow \frac{i}{2\sqrt{3}}, \{12, 52\} \rightarrow \frac{i}{2\sqrt{3}}, \{13, 13\} \rightarrow -\frac{1}{2}, \{13, 25\} \rightarrow \frac{1}{2}, \{13, 37\} \rightarrow \frac{1}{2}, \{13, 49\} \rightarrow -\frac{1}{2}, \{14, 14\} \rightarrow -\frac{1}{2}, \\
& \{14, 26\} \rightarrow \frac{1}{2}, \{14, 38\} \rightarrow \frac{1}{2}, \{14, 50\} \rightarrow -\frac{1}{2}, \{15, 15\} \rightarrow -\frac{1}{2}, \{15, 27\} \rightarrow \frac{1}{2}, \{15, 39\} \rightarrow \frac{1}{2}, \{15, 51\} \rightarrow -\frac{1}{2}, \{16, 16\} \rightarrow -\frac{1}{2}, \\
& \{16, 28\} \rightarrow \frac{1}{2}, \{16, 40\} \rightarrow \frac{1}{2}, \{16, 52\} \rightarrow -\frac{1}{2}, \{17, 29\} \rightarrow \frac{1}{\sqrt{6}}, \{17, 53\} \rightarrow \frac{1}{\sqrt{6}}, \{17, 63\} \rightarrow \sqrt{\frac{2}{3}}, \{18, 13\} \rightarrow -\frac{1}{3\sqrt{2}}, \\
& \{18, 25\} \rightarrow -\frac{1}{3\sqrt{2}}, \{18, 30\} \rightarrow \frac{1}{3\sqrt{2}}, \{18, 37\} \rightarrow -\frac{1}{3\sqrt{2}}, \{18, 47\} \rightarrow -\frac{\sqrt{2}}{3}, \{18, 49\} \rightarrow -\frac{1}{3\sqrt{2}}, \{18, 54\} \rightarrow \frac{1}{3\sqrt{2}}, \\
& \{18, 59\} \rightarrow -\frac{\sqrt{2}}{3}, \{18, 64\} \rightarrow \frac{\sqrt{2}}{3}, \{19, 21\} \rightarrow -\sqrt{\frac{2}{3}}, \{19, 31\} \rightarrow -\frac{1}{\sqrt{6}}, \{19, 55\} \rightarrow -\frac{1}{\sqrt{6}}, \{20, 5\} \rightarrow \frac{\sqrt{2}}{3}, \{20, 15\} \rightarrow \frac{1}{3\sqrt{2}}, \\
& \{20, 17\} \rightarrow \frac{\sqrt{2}}{3}, \{20, 22\} \rightarrow -\frac{\sqrt{2}}{3}, \{20, 27\} \rightarrow \frac{1}{3\sqrt{2}}, \{20, 32\} \rightarrow -\frac{1}{3\sqrt{2}}, \{20, 39\} \rightarrow \frac{1}{3\sqrt{2}}, \{20, 51\} \rightarrow \frac{1}{3\sqrt{2}}, \\
& \{20, 56\} \rightarrow -\frac{1}{3\sqrt{2}}, \{21, 9\} \rightarrow \frac{1}{3\sqrt{2}}, \{21, 14\} \rightarrow -\frac{1}{3\sqrt{2}}, \{21, 26\} \rightarrow -\frac{1}{3\sqrt{2}}, \{21, 33\} \rightarrow \frac{1}{3\sqrt{2}}, \{21, 38\} \rightarrow -\frac{1}{3\sqrt{2}}, \\
& \{21, 43\} \rightarrow \frac{\sqrt{2}}{3}, \{21, 48\} \rightarrow -\frac{\sqrt{2}}{3}, \{21, 50\} \rightarrow -\frac{1}{3\sqrt{2}}, \{21, 60\} \rightarrow -\frac{\sqrt{2}}{3}, \{22, 10\} \rightarrow \frac{1}{\sqrt{6}}, \{22, 34\} \rightarrow \frac{1}{\sqrt{6}}, \{22, 44\} \rightarrow \sqrt{\frac{2}{3}}, \\
& \{23, 1\} \rightarrow -\frac{\sqrt{2}}{3}, \{23, 6\} \rightarrow \frac{\sqrt{2}}{3}, \{23, 11\} \rightarrow -\frac{1}{3\sqrt{2}}, \{23, 16\} \rightarrow \frac{1}{3\sqrt{2}}, \{23, 18\} \rightarrow \frac{\sqrt{2}}{3}, \{23, 28\} \rightarrow \frac{1}{3\sqrt{2}}, \{23, 35\} \rightarrow -\frac{1}{3\sqrt{2}}, \\
& \{23, 40\} \rightarrow \frac{1}{3\sqrt{2}}, \{23, 52\} \rightarrow \frac{1}{3\sqrt{2}}, \{24, 2\} \rightarrow -\sqrt{\frac{2}{3}}, \{24, 12\} \rightarrow -\frac{1}{\sqrt{6}}, \{24, 36\} \rightarrow -\frac{1}{\sqrt{6}}, \{25, 29\} \rightarrow \frac{i}{\sqrt{2}}, \{25, 53\} \rightarrow -\frac{i}{\sqrt{2}}, \\
& \{26, 13\} \rightarrow -\frac{i}{\sqrt{6}}, \{26, 25\} \rightarrow -\frac{i}{\sqrt{6}}, \{26, 30\} \rightarrow \frac{i}{\sqrt{6}}, \{26, 37\} \rightarrow \frac{i}{\sqrt{6}}, \{26, 49\} \rightarrow \frac{i}{\sqrt{6}}, \{26, 54\} \rightarrow -\frac{i}{\sqrt{6}}, \{27, 31\} \rightarrow \frac{i}{\sqrt{2}}, \\
& \{27, 55\} \rightarrow -\frac{i}{\sqrt{2}}, \{28, 15\} \rightarrow -\frac{i}{\sqrt{6}}, \{28, 27\} \rightarrow -\frac{i}{\sqrt{6}}, \{28, 32\} \rightarrow \frac{i}{\sqrt{6}}, \{28, 39\} \rightarrow \frac{i}{\sqrt{6}}, \{28, 51\} \rightarrow \frac{i}{\sqrt{6}}, \{28, 56\} \rightarrow -\frac{i}{\sqrt{6}},
\end{aligned}$$

$$\begin{aligned}
& \{29, 9\} \rightarrow \frac{i}{\sqrt{6}}, \{29, 14\} \rightarrow -\frac{i}{\sqrt{6}}, \{29, 26\} \rightarrow -\frac{i}{\sqrt{6}}, \{29, 33\} \rightarrow -\frac{i}{\sqrt{6}}, \{29, 38\} \rightarrow \frac{i}{\sqrt{6}}, \{29, 50\} \rightarrow \frac{i}{\sqrt{6}}, \{30, 10\} \rightarrow \frac{i}{\sqrt{2}}, \\
& \{30, 34\} \rightarrow -\frac{i}{\sqrt{2}}, \{31, 11\} \rightarrow \frac{i}{\sqrt{6}}, \{31, 16\} \rightarrow -\frac{i}{\sqrt{6}}, \{31, 28\} \rightarrow -\frac{i}{\sqrt{6}}, \{31, 35\} \rightarrow -\frac{i}{\sqrt{6}}, \{31, 40\} \rightarrow \frac{i}{\sqrt{6}}, \{31, 52\} \rightarrow \frac{i}{\sqrt{6}}, \\
& \{32, 12\} \rightarrow \frac{i}{\sqrt{2}}, \{32, 36\} \rightarrow -\frac{i}{\sqrt{2}}, \{33, 45\} \rightarrow \frac{1}{\sqrt{6}}, \{33, 57\} \rightarrow \frac{1}{\sqrt{6}}, \{33, 62\} \rightarrow \sqrt{\frac{2}{3}}, \{34, 41\} \rightarrow -\sqrt{\frac{2}{3}}, \{34, 46\} \rightarrow -\frac{1}{\sqrt{6}}, \\
& \{34, 58\} \rightarrow -\frac{1}{\sqrt{6}}, \{35, 13\} \rightarrow -\frac{1}{3\sqrt{2}}, \{35, 25\} \rightarrow -\frac{1}{3\sqrt{2}}, \{35, 30\} \rightarrow -\frac{\sqrt{2}}{3}, \{35, 37\} \rightarrow -\frac{1}{3\sqrt{2}}, \{35, 47\} \rightarrow \frac{1}{3\sqrt{2}}, \\
& \{35, 49\} \rightarrow -\frac{1}{3\sqrt{2}}, \{35, 54\} \rightarrow -\frac{\sqrt{2}}{3}, \{35, 59\} \rightarrow \frac{1}{3\sqrt{2}}, \{35, 64\} \rightarrow \frac{\sqrt{2}}{3}, \{36, 9\} \rightarrow \frac{\sqrt{2}}{3}, \{36, 14\} \rightarrow \frac{1}{3\sqrt{2}}, \{36, 26\} \rightarrow \frac{1}{3\sqrt{2}}, \\
& \{36, 33\} \rightarrow \frac{\sqrt{2}}{3}, \{36, 38\} \rightarrow \frac{1}{3\sqrt{2}}, \{36, 43\} \rightarrow -\frac{\sqrt{2}}{3}, \{36, 48\} \rightarrow -\frac{1}{3\sqrt{2}}, \{36, 50\} \rightarrow \frac{1}{3\sqrt{2}}, \{36, 60\} \rightarrow -\frac{1}{3\sqrt{2}}, \\
& \{37, 5\} \rightarrow \frac{1}{3\sqrt{2}}, \{37, 15\} \rightarrow -\frac{1}{3\sqrt{2}}, \{37, 17\} \rightarrow \frac{1}{3\sqrt{2}}, \{37, 22\} \rightarrow \frac{\sqrt{2}}{3}, \{37, 27\} \rightarrow -\frac{1}{3\sqrt{2}}, \{37, 32\} \rightarrow -\frac{\sqrt{2}}{3}, \\
& \{37, 39\} \rightarrow -\frac{1}{3\sqrt{2}}, \{37, 51\} \rightarrow -\frac{1}{3\sqrt{2}}, \{37, 56\} \rightarrow -\frac{\sqrt{2}}{3}, \{38, 1\} \rightarrow -\frac{\sqrt{2}}{3}, \{38, 6\} \rightarrow -\frac{1}{3\sqrt{2}}, \{38, 11\} \rightarrow \frac{\sqrt{2}}{3}, \\
& \{38, 16\} \rightarrow \frac{1}{3\sqrt{2}}, \{38, 18\} \rightarrow -\frac{1}{3\sqrt{2}}, \{38, 28\} \rightarrow \frac{1}{3\sqrt{2}}, \{38, 35\} \rightarrow \frac{\sqrt{2}}{3}, \{38, 40\} \rightarrow \frac{1}{3\sqrt{2}}, \{38, 52\} \rightarrow \frac{1}{3\sqrt{2}}, \{39, 7\} \rightarrow \frac{1}{\sqrt{6}}, \\
& \{39, 19\} \rightarrow \frac{1}{\sqrt{6}}, \{39, 24\} \rightarrow \sqrt{\frac{2}{3}}, \{40, 3\} \rightarrow -\sqrt{\frac{2}{3}}, \{40, 8\} \rightarrow -\frac{1}{\sqrt{6}}, \{40, 20\} \rightarrow -\frac{1}{\sqrt{6}}, \{41, 45\} \rightarrow \frac{i}{\sqrt{2}}, \{41, 57\} \rightarrow -\frac{i}{\sqrt{2}}, \\
& \{42, 46\} \rightarrow \frac{i}{\sqrt{2}}, \{42, 58\} \rightarrow -\frac{i}{\sqrt{2}}, \{43, 13\} \rightarrow -\frac{i}{\sqrt{6}}, \{43, 25\} \rightarrow \frac{i}{\sqrt{6}}, \{43, 37\} \rightarrow -\frac{i}{\sqrt{6}}, \{43, 47\} \rightarrow \frac{i}{\sqrt{6}}, \{43, 49\} \rightarrow \frac{i}{\sqrt{6}}, \\
& \{43, 59\} \rightarrow -\frac{i}{\sqrt{6}}, \{44, 14\} \rightarrow -\frac{i}{\sqrt{6}}, \{44, 26\} \rightarrow \frac{i}{\sqrt{6}}, \{44, 38\} \rightarrow -\frac{i}{\sqrt{6}}, \{44, 48\} \rightarrow \frac{i}{\sqrt{6}}, \{44, 50\} \rightarrow \frac{i}{\sqrt{6}}, \{44, 60\} \rightarrow -\frac{i}{\sqrt{6}}, \\
& \{45, 5\} \rightarrow \frac{i}{\sqrt{6}}, \{45, 15\} \rightarrow -\frac{i}{\sqrt{6}}, \{45, 17\} \rightarrow -\frac{i}{\sqrt{6}}, \{45, 27\} \rightarrow \frac{i}{\sqrt{6}}, \{45, 39\} \rightarrow -\frac{i}{\sqrt{6}}, \{45, 51\} \rightarrow \frac{i}{\sqrt{6}}, \{46, 6\} \rightarrow \frac{i}{\sqrt{6}}, \\
& \{46, 16\} \rightarrow -\frac{i}{\sqrt{6}}, \{46, 18\} \rightarrow -\frac{i}{\sqrt{6}}, \{46, 28\} \rightarrow \frac{i}{\sqrt{6}}, \{46, 40\} \rightarrow -\frac{i}{\sqrt{6}}, \{46, 52\} \rightarrow \frac{i}{\sqrt{6}}, \{47, 7\} \rightarrow \frac{i}{\sqrt{2}}, \{47, 19\} \rightarrow -\frac{i}{\sqrt{2}}, \\
& \{48, 8\} \rightarrow \frac{i}{\sqrt{2}}, \{48, 20\} \rightarrow -\frac{i}{\sqrt{2}}, \{49, 61\} \rightarrow 1, \{50, 45\} \rightarrow -\frac{1}{\sqrt{3}}, \{50, 57\} \rightarrow -\frac{1}{\sqrt{3}}, \{50, 62\} \rightarrow \frac{1}{\sqrt{3}}, \{51, 29\} \rightarrow -\frac{1}{\sqrt{3}}, \\
& \{51, 53\} \rightarrow -\frac{1}{\sqrt{3}}, \{51, 63\} \rightarrow \frac{1}{\sqrt{3}}, \{52, 13\} \rightarrow \frac{1}{3}, \{52, 25\} \rightarrow \frac{1}{3}, \{52, 30\} \rightarrow -\frac{1}{3}, \{52, 37\} \rightarrow \frac{1}{3}, \{52, 47\} \rightarrow -\frac{1}{3}, \\
& \{52, 49\} \rightarrow \frac{1}{3}, \{52, 54\} \rightarrow -\frac{1}{3}, \{52, 59\} \rightarrow -\frac{1}{3}, \{52, 64\} \rightarrow \frac{1}{3}, \{53, 21\} \rightarrow \frac{1}{\sqrt{3}}, \{53, 31\} \rightarrow -\frac{1}{\sqrt{3}}, \{53, 55\} \rightarrow -\frac{1}{\sqrt{3}}, \\
& \{54, 5\} \rightarrow -\frac{1}{3}, \{54, 15\} \rightarrow \frac{1}{3}, \{54, 17\} \rightarrow -\frac{1}{3}, \{54, 22\} \rightarrow \frac{1}{3}, \{54, 27\} \rightarrow \frac{1}{3}, \{54, 32\} \rightarrow -\frac{1}{3}, \{54, 39\} \rightarrow \frac{1}{3}, \{54, 51\} \rightarrow \frac{1}{3}, \\
& \{54, 56\} \rightarrow -\frac{1}{3}, \{55, 23\} \rightarrow 1, \{56, 7\} \rightarrow -\frac{1}{\sqrt{3}}, \{56, 19\} \rightarrow -\frac{1}{\sqrt{3}}, \{56, 24\} \rightarrow \frac{1}{\sqrt{3}}, \{57, 41\} \rightarrow \frac{1}{\sqrt{3}}, \{57, 46\} \rightarrow -\frac{1}{\sqrt{3}}, \\
& \{57, 58\} \rightarrow -\frac{1}{\sqrt{3}}, \{58, 42\} \rightarrow 1, \{59, 9\} \rightarrow -\frac{1}{3}, \{59, 14\} \rightarrow \frac{1}{3}, \{59, 26\} \rightarrow \frac{1}{3}, \{59, 33\} \rightarrow -\frac{1}{3}, \{59, 38\} \rightarrow \frac{1}{3}, \{59, 43\} \rightarrow \frac{1}{3}, \\
& \{59, 48\} \rightarrow -\frac{1}{3}, \{59, 50\} \rightarrow \frac{1}{3}, \{59, 60\} \rightarrow -\frac{1}{3}, \{60, 10\} \rightarrow -\frac{1}{\sqrt{3}}, \{60, 34\} \rightarrow -\frac{1}{\sqrt{3}}, \{60, 44\} \rightarrow \frac{1}{\sqrt{3}}, \{61, 1\} \rightarrow \frac{1}{3}, \\
& \{61, 6\} \rightarrow -\frac{1}{3}, \{61, 11\} \rightarrow -\frac{1}{3}, \{61, 16\} \rightarrow \frac{1}{3}, \{61, 18\} \rightarrow -\frac{1}{3}, \{61, 28\} \rightarrow \frac{1}{3}, \{61, 35\} \rightarrow -\frac{1}{3}, \{61, 40\} \rightarrow \frac{1}{3}, \{61, 52\} \rightarrow \frac{1}{3}, \\
& \{62, 2\} \rightarrow \frac{1}{\sqrt{3}}, \{62, 12\} \rightarrow -\frac{1}{\sqrt{3}}, \{62, 36\} \rightarrow -\frac{1}{\sqrt{3}}, \{63, 3\} \rightarrow \frac{1}{\sqrt{3}}, \{63, 8\} \rightarrow -\frac{1}{\sqrt{3}}, \{63, 20\} \rightarrow -\frac{1}{\sqrt{3}}, \{64, 4\} \rightarrow 1.
\end{aligned}$$

Supplemental Material E: Semidefinite program for optimal average PPT purification fidelity

Definition 4 For a given pure state set \mathcal{S} , noise channel \mathcal{N} and the average success probability \bar{P} , the optimal $n \rightarrow 1$ average PPT purification fidelity is defined by

$$\bar{F}_{\text{PPT}}^*(n, \bar{P}; \mathcal{S}, \mathcal{N}) = \max_{\mathcal{E}} \{ \bar{F}(n; \mathcal{S}, \mathcal{N}, \mathcal{E}) \mid \mathcal{E} \in \text{PPT} \cap \text{CPTN}, \frac{1}{|\mathcal{S}|} \sum_{\psi \in \mathcal{S}} \text{Tr}[\mathcal{E}(\mathcal{N}(\psi)^{\otimes n})] = \bar{P} \}. \quad (\text{E.1})$$

Proposition 8 For a given pure state set \mathcal{S} , noise channel \mathcal{N} , and the average success probability \bar{P} , the optimal purification fidelity achieved by the $n \rightarrow 1$ PPT purification protocol \mathcal{E} can be characterized by the following SDP.

$$\bar{F}_{\text{PPT}}^*(n, \bar{P}; \mathcal{S}, \mathcal{N}) = \max \frac{1}{\bar{P}} \text{Tr}[Q_{A^n B^n A' B'} J_{\mathcal{E}_{A^n B^n A' B'}}^{T_{A^n B^n}}]; \quad (\text{E.2a})$$

$$\text{s.t. } \text{Tr}[R_{A^n B^n A' B'} J_{\mathcal{E}_{A^n B^n A' B'}}^{T_{A^n B^n}}] = \bar{P}; \quad (\text{E.2b})$$

$$J_{\mathcal{E}_{A^n B^n A' B'}} \geq 0; \quad \text{Tr}_{A' B'} [J_{\mathcal{E}_{A^n B^n A' B'}}] \leq I_{A^n B^n}; \quad (\text{E.2c})$$

$$J_{\mathcal{E}_{A^n B^n A' B'}}^{T_{A^n A'}} \geq 0, \quad (\text{E.2d})$$

$$\frac{\text{Tr}[J_{\mathcal{E}_{A^n B^n A' B'}}^{T_{A^n B^n}} \mathcal{N}^{\otimes n} \otimes \mathcal{I}(\psi_i^{\otimes n+1})]}{\text{Tr}[J_{\mathcal{E}_{A^n B^n A' B'}}^{T_{A^n B^n}} \mathcal{N}^{\otimes n}(\psi_i^{\otimes n}) \otimes I_{A' B'}]} \geq \text{Tr}[\psi_i \mathcal{N}(\psi_i)] \quad \forall \psi_i \in \mathcal{S}, \quad (\text{E.2e})$$

where $J_{\mathcal{E}_{A^n B^n A' B'}}$ is the Choi-Jamiołkowski matrix of map \mathcal{E} , T refers to the transpose operation. In addition

$$Q_{A^n B^n A' B'} = \frac{1}{|\mathcal{S}|} \sum_{\psi_i \in \mathcal{S}} \mathcal{N}^{\otimes n} \otimes \mathcal{I}(\psi_i^{\otimes n+1}) \quad (\text{E.3})$$

$$R_{A^n B^n A' B'} = \frac{1}{|\mathcal{S}|} \sum_{\psi_i \in \mathcal{S}} \mathcal{N}^{\otimes n}(\psi_i^{\otimes n}) \otimes I \quad (\text{E.4})$$

where $|\mathcal{S}|$ is the size of the set \mathcal{S} , \mathcal{I} and I refers to identity channel and identity matrix, respectively.

Proof The objective function of the primal SDP is

$$\frac{1}{\bar{P}|\mathcal{S}|} \sum_{\psi_i \in \mathcal{S}} \text{Tr}[\psi_i \bar{\rho}_i] = \frac{1}{\bar{P}|\mathcal{S}|} \sum_{\psi_i \in \mathcal{S}} \text{Tr}[\psi_i \mathcal{E}(\mathcal{N}(\psi_i)^{\otimes n})] \quad (\text{E.5})$$

$$= \frac{1}{\bar{P}|\mathcal{S}|} \sum_{\psi_i \in \mathcal{S}} \text{Tr} \left[J_{\mathcal{E}_{A^n B^n A' B'}}^{T_{A^n B^n}} \mathcal{N}(\psi_i)^{\otimes n} \otimes \psi_i \right] \quad (\text{E.6})$$

$$= \frac{1}{\bar{P}} \text{Tr} \left[J_{\mathcal{E}_{A^n B^n A' B'}}^{T_{A^n B^n}} \sum_{\psi_i \in \mathcal{S}} \frac{1}{|\mathcal{S}|} \mathcal{N}^{\otimes n} \otimes \mathcal{I}(\psi_i^{\otimes n+1}) \right] \quad (\text{E.7})$$

$$= \frac{1}{\bar{P}} \text{Tr} \left[Q_{A^n B^n A' B'} J_{\mathcal{E}_{A^n B^n A' B'}}^{T_{A^n B^n}} \right]. \quad (\text{E.8})$$

Similarly, we arrive at the average success probability constraint as shown in Eq. (E.2b). Eq. (E.2c) and Eq. (E.2d) ensure the purification protocol \mathcal{E} satisfies CPTN and PPT constraints, respectively. Eq. (E.2e) guarantees that for every state in the set \mathcal{S} , the purified state by the CPTN map \mathcal{E} is less noisy. \blacksquare

1. Dual problem

According to the primal problem, we have the Lagrange function

$$\begin{aligned} & \mathcal{L}(J_{\mathcal{E}_{A^n B^n A' B'}}, x, K_{A^n B^n}, L_{A^n B^n A' B'}, y_1, y_2, \dots, y_{|\mathcal{S}|}) \\ &= \frac{1}{\bar{P}} \text{Tr}[Q_{A^n B^n A' B'} J_{\mathcal{E}_{A^n B^n A' B'}}^{T_{A^n B^n}}] + x \langle \text{Tr}[R_{A^n B^n A' B'} J_{\mathcal{E}_{A^n B^n A' B'}}^{T_{A^n B^n}}] - \bar{P} \rangle + \langle K_{A^n B^n}, I_{A^n B^n} - \text{Tr}_{A' B'} [J_{\mathcal{E}_{A^n B^n A' B'}}] \rangle \\ & \quad + \langle L_{A^n B^n A' B'}, J_{\mathcal{E}_{A^n B^n A' B'}}^{T_{A^n A'}} \rangle + \sum_{\psi_i \in \mathcal{S}} y_i \left(\text{Tr}[J_{\mathcal{E}_{A^n B^n A' B'}}^{T_{A^n B^n}} \mathcal{N}^{\otimes n} \otimes \mathcal{I}(\psi_i^{\otimes n+1})] \right) \end{aligned}$$

$$- \sum_{\psi_i \in \mathcal{S}} y_i \left(\text{Tr}[\psi_i \mathcal{N}(\psi_i)] \text{Tr}[J_{\mathcal{E}_{A^n B^n A' B'}}^{T_{A^n B^n}} \mathcal{N}^{\otimes n}(\psi_i^{\otimes n}) \otimes I_{A' B'}] \right) \quad (\text{E.9})$$

$$= -\bar{P}x + \langle K_{A^n B^n} \rangle + \left\langle J_{\mathcal{E}_{A^n B^n A' B'}} + \frac{1}{p} Q_{A^n B^n A' B'}^{T_{A^n B^n}} + x R_{A^n B^n A' B'}^{T_{A^n B^n}} - K_{A^n B^n} \otimes I_{A' B'} + L_{A^n B^n A' B'}^{T_{A^n A'}} \right. \\ \left. + \sum_{\psi_i \in \mathcal{S}} y_i \mathcal{N}^{\otimes n} \otimes \mathcal{I}(\psi_i^{\otimes n+1})^{T_{A^n B^n}} - \sum_{\psi_i \in \mathcal{S}} y_i \text{Tr}[\psi_i \mathcal{N}(\psi_i)] \mathcal{N}^{\otimes n}(\psi_i^{\otimes n})^T \otimes I_{A' B'} \right\rangle, \quad (\text{E.10})$$

where $x, K_{A^n B^n}, L_{A^n B^n A' B'}, y_1, \dots, y_{|\mathcal{S}|}$ are Lagrange multipliers. The Lagrange dual function is

$$g(x, K_{A^n B^n}, L_{A^n B^n A' B'}, \mathbf{y}) = \sup_{J_{\mathcal{E}} \geq 0} \mathcal{L}(J_{\mathcal{E}_{A^n B^n A' B'}}^{T_{A^n B^n}}, x, K_{A^n B^n}, L_{A^n B^n A' B'}, \mathbf{y}),$$

where $\mathbf{y} = [y_1, y_2, \dots, y_{|\mathcal{S}|}]$. The variables must satisfy $K_{A^n B^n} \geq 0, L_{A^n B^n A' B'} \geq 0$, and $\mathbf{y} \geq 0$. Otherwise, there is no feasible solution to the primal problem. Besides, since $J_{\mathcal{E}_{A^n B^n}} \geq 0$, it holds that

$$\frac{1}{\bar{P}} Q_{A^n B^n A' B'}^{T_{A^n B^n}} + x R_{A^n B^n A' B'}^{T_{A^n B^n}} - K_{A^n B^n} \otimes I_{A' B'} + L_{A^n B^n A' B'}^{T_{A^n A'}} + \sum_{\psi_i \in \mathcal{S}} y_i \mathcal{N}^{\otimes n} \otimes \mathcal{I}(\psi_i^{\otimes n+1})^{T_{A^n B^n}} \\ - \sum_{\psi_i \in \mathcal{S}} y_i \text{Tr}[\psi_i \mathcal{N}(\psi_i)] \mathcal{N}^{\otimes n}(\psi_i^{\otimes n})^T \otimes I_{A' B'} \leq 0, \quad (\text{E.11})$$

otherwise the dual problem is unbounded. Thus, we arrive at the dual SDP as

$$\min \langle K_{A^n B^n} \rangle - \bar{P}x \quad (\text{E.12a})$$

$$\text{s.t. } K_{A^n B^n} \geq 0; L_{A^n B^n A' B'} \geq 0; \mathbf{y} \geq 0; \quad (\text{E.12b})$$

$$\frac{1}{\bar{P}} Q_{A^n B^n A' B'}^{T_{A^n B^n}} + x R_{A^n B^n A' B'}^{T_{A^n B^n}} - K_{A^n B^n} \otimes I_{A' B'} + L_{A^n B^n A' B'}^{T_{A^n A'}} + \sum_{\psi_i \in \mathcal{S}} y_i \mathcal{N}^{\otimes n} \otimes \mathcal{I}(\psi_i^{\otimes n+1})^{T_{A^n B^n}} \\ - \sum_{\psi_i \in \mathcal{S}} y_i \text{Tr}[\psi_i \mathcal{N}(\psi_i)] \mathcal{N}^{\otimes n}(\psi_i^{\otimes n})^T \otimes I_{A' B'} \leq 0. \quad (\text{E.12c})$$

Supplemental Material F: Equivalence between global and local depolarizing noises

Lemma 9 Applying depolarizing channels locally on maximally entangled states $\mathcal{N}_A^{\gamma_1} \otimes \mathcal{N}_B^{\gamma_2}$ is equivalent to applying global depolarizing channel $\mathcal{N}_{AB}^{\gamma'}$ with parameter $\gamma' = 1 - (1 - \gamma_1)(1 - \gamma_2)$.

Proof Denote Φ_{AB}^{MAX} as an arbitrary maximally entangled state. Due to the property of maximally entangled states, the partial traced density matrix is $\rho_A = \rho_B = I/d$, where d is the dimension of the subsystems A and B , i.e., $d_A = d_B = d$. When apply the local depolarizing noise to Φ_{AB}^{MAX} , we have

$$\begin{aligned} \mathcal{N}_A^{\gamma_1} \otimes \mathcal{N}_B^{\gamma_2}(\Phi_{AB}^{MAX}) &= (1 - \gamma_1)(1 - \gamma_2)\Phi_{AB}^{MAX} + \gamma_1(1 - \gamma_2)\frac{I_{AB}}{d_{AB}} + \gamma_2(1 - \gamma_1)\frac{I_{AB}}{d_{AB}} + \gamma_1\gamma_2\frac{I_{AB}}{d_{AB}} \\ &= (1 - \gamma_1)(1 - \gamma_2)\Phi_{AB}^{MAX} + (\gamma_1 + \gamma_2 - \gamma_1\gamma_2)\frac{I_{AB}}{d_{AB}} \\ &= (1 - \gamma_1)(1 - \gamma_2)\Phi_{AB}^{MAX} + (1 - (1 - \gamma_1)(1 - \gamma_2))\frac{I_{AB}}{d_{AB}} \\ &= (1 - \gamma')\Phi_{AB}^{MAX} + \gamma'\frac{I_{AB}}{d_{AB}} \\ &= \mathcal{N}_{AB}^{\gamma'}(\Phi_{AB}^{MAX}), \end{aligned} \quad (\text{F.1})$$

where $\gamma' = 1 - (1 - \gamma_1)(1 - \gamma_2)$. The proof is completed. ■

Supplemental Material G: Proof of Theorem 2

Theorem 2 (No-go theorem for four Bell states) *For the local depolarizing noise channel $\mathcal{N}_{AB}^{\gamma_1, \gamma_2}$ with noise levels γ_1 and γ_2 , there is no nontrivial $2 \rightarrow 1$ LOCC purification protocol for the set that contains 4 Bell states \mathcal{S}_B .*

Proof Note that arbitrary four orthogonal maximally entangled pure states can be achieved by applying local unitaries on the four Bell states. Thus, it is equivalent to proving there is no nontrivial purification protocol for the set that contains four Bell states $\mathcal{S}_B = \{\Phi^+, \Phi^-, \Psi^+, \Psi^-\}$.

The main idea of this proof is to show that the optimal $2 \rightarrow 1$ PPT protocol is trivial, and since LOCC is a subset of PPT operations, we arrive at the no-go theorem for the LOCC protocol. From Proposition 8, the optimal fidelity can be achieved by the following SDP.

$$\bar{F}_{\text{PPT}}^*(n = 2, \bar{P}; \mathcal{S}_B, \mathcal{N}_{AB}^{\gamma_1, \gamma_2}) = \max \frac{1}{\bar{P}} \text{Tr}[Q_{A^n B^n A' B'} J_{\mathcal{E}_{A^n B^n A' B'}}^{T_{A^n B^n}}]; \quad (\text{G.1a})$$

$$\text{s.t. } \text{Tr}[R_{A^n B^n A' B'} J_{\mathcal{E}_{A^n B^n A' B'}}^{T_{A^n B^n}}] = \bar{P}; \quad (\text{G.1b})$$

$$J_{\mathcal{E}_{A^n B^n A' B'}} \geq 0; \quad \text{Tr}_{A' B'}[J_{\mathcal{E}_{A^n B^n A' B'}}] \leq I_{A^n B^n}; \quad (\text{G.1c})$$

$$J_{\mathcal{E}_{A^n B^n A' B'}}^{T_{A^n A'}} \geq 0; \quad (\text{G.1d})$$

$$\frac{\text{Tr}[J_{\mathcal{E}_{A^n B^n A' B'}}^{T_{A^n B^n}} \mathcal{N}_{AB}^{\gamma_1, \gamma_2 \otimes n} \otimes \mathcal{I}(\psi_i^{\otimes n+1})]}{\text{Tr}[J_{\mathcal{E}_{A^n B^n A' B'}}^{T_{A^n B^n}} \mathcal{N}_{AB}^{\gamma_1, \gamma_2 \otimes n}(\psi_i^{\otimes n}) \otimes I_{A' B'}]} \geq \text{Tr}[\psi_i \mathcal{N}(\psi_i)] \quad \forall \psi_i \in \mathcal{S}_B, \quad (\text{G.1e})$$

where $Q_{A^n B^n A' B'} = \frac{1}{|\mathcal{S}_B|} \sum_{\psi_i \in \mathcal{S}_B} \mathcal{N}_{AB}^{\gamma_1, \gamma_2 \otimes 2} \otimes \mathcal{I}(\psi_i^{\otimes 3})$ and $R_{A^n B^n A' B'} = \frac{1}{|\mathcal{S}_B|} \sum_{\psi_i \in \mathcal{S}_B} \mathcal{N}_{AB}^{\gamma_1, \gamma_2 \otimes 2}(\psi_i^{\otimes 2})_{A^n B^n} \otimes I_{A' B'}$. The noise channel \mathcal{N} is local depolarizing channel, i.e., $\mathcal{N}_{AB}^{\gamma_1, \gamma_2} = \mathcal{N}_A^{\gamma_1} \otimes \mathcal{N}_B^{\gamma_2}$. Since the input states are all maximally entangled states, according to Lemma 9, it is equivalent to replace the local depolarizing noise channel with the global depolarizing channel, which is $\mathcal{N}_{AB}^{\gamma_1, \gamma_2} = \mathcal{N}_{AB}^{\gamma'}$ with $\gamma' = 1 - (1 - \gamma_1)(1 - \gamma_2)$. Obviously, the partial trace channel, is one feasible solution to the primal SDP, i.e.,

$$J_{\mathcal{E}_{A^n B^n A' B'}} = \bar{P} \cdot \Phi_{A_1 A'}^+ \otimes \Phi_{B_1 B'}^+ \otimes I_{A^n B^n / A_1 B_1}. \quad (\text{G.2})$$

In this case, we have

$$\bar{F}_{\text{PPT}}^*(2, \bar{P}; \mathcal{S}_B, \mathcal{N}_{AB}^{\gamma'}) \geq 1 - \frac{3}{4}\gamma', \quad (\text{G.3})$$

which is the same as the average fidelity without purification, implying the partial trace channel is a trivial solution.

Besides, we also need to prove $\bar{F}_{\text{PPT}}^*(n, \bar{P}; \mathcal{S}_B, \mathcal{N}_{AB}^{\gamma'}) \leq 1 - \frac{3}{4}\gamma'$ by the following dual SDP.

$$\min \langle K_{A^n B^n} \rangle - \bar{P}x \quad (\text{G.4a})$$

$$\text{s.t. } K_{A^n B^n} \geq 0; \quad L_{A^n B^n A' B'} \geq 0; \quad y_i \geq 0, \quad \forall i; \quad (\text{G.4b})$$

$$\begin{aligned} & \frac{1}{\bar{P}} Q_{A^n B^n A' B'}^{T_{A^n B^n}} + x R_{A^n B^n A' B'}^{T_{A^n B^n}} - K_{A^n B^n} \otimes I_{A' B'} + L_{A^n B^n A' B'}^{T_{A^n A'}} \\ & + \sum_{\psi_i \in \mathcal{S}_B} y_i \mathcal{N}_{AB}^{\gamma' \otimes n} \otimes \mathcal{I}(\psi_i^{\otimes n+1})^{T_{A^n B^n}} - \sum_{\psi_i \in \mathcal{S}_B} y_i \text{Tr}[\psi_i \mathcal{N}_{AB}^{\gamma'}(\psi_i)] \mathcal{N}_{AB}^{\gamma' \otimes n}(\psi_i^{\otimes n})^T \otimes I_{A' B'} \leq 0. \end{aligned} \quad (\text{G.4c})$$

We note that

$$K_{A^n B^n} = 0; \quad x = -\frac{1}{\bar{P}} \left(1 - \frac{3}{4}\gamma'\right); \quad y_i = 0, \quad \forall i; \quad (\text{G.5a})$$

$$\begin{aligned} L_{A^n B^n A' B'} = & \frac{\gamma'(1 - \gamma')(1 - 3\gamma'/4)}{8\bar{P}} [(\Phi_{A_1 B_1}^+ \Phi_{A_2 B_2}^- + \Phi_{A_1 B_1}^- \Phi_{A_2 B_2}^+)(\Psi^+ + \Psi^-)_{A' B'} \\ & + (\Psi_{A_1 B_1}^+ \Psi_{A_2 B_2}^- + \Psi_{A_1 B_1}^- \Psi_{A_2 B_2}^+)(\Phi^+ + \Phi^-)_{A' B'} \\ & + (\Phi_{A_1 B_1}^+ \Phi_{A' B'}^- + \Phi_{A_1 B_1}^- \Phi_{A' B'}^+)(\Psi^+ + \Psi^-)_{A_2 B_2} \\ & + (\Psi_{A_1 B_1}^+ \Psi_{A' B'}^- + \Psi_{A_1 B_1}^- \Psi_{A' B'}^+)(\Phi^+ + \Phi^-)_{A_2 B_2} \\ & + (\Phi_{A_2 B_2}^+ \Phi_{A' B'}^- + \Phi_{A_2 B_2}^- \Phi_{A' B'}^+)(\Psi^+ + \Psi^-)_{A_1 B_1} \end{aligned}$$

$$+(\Psi_{A_2 B_2}^+ \Psi_{A' B'}^- + \Psi_{A_2 B_2}^- \Psi_{A' B'}^+)(\Phi^+ + \Phi^-)_{A_1 B_1}], \quad (\text{G.5b})$$

is a feasible solution to the dual SDP. The constraints in Eq. (G.4b) can be easily checked. For the constraint shown in Eq. (G.4c), substitute $L_{A^n B^n A' B'}$ into the left hand side of (G.4c), and the largest non-zero eigenvalue is $\frac{\gamma'(\gamma'-1)}{16P} \leq 0$ when $0 \leq \gamma' \leq 1$. Thus, Eq. (G.5) is a feasible solution to the dual SDP, and we have $\bar{F}_{\text{PPT}}^*(2, \bar{P}; \mathcal{S}_B, \mathcal{N}_{AB}^{\gamma'}) \leq 1 - \frac{3}{4}\gamma'$. Combing with Eq. (G.3), we have

$$\bar{F}_{\text{PPT}}^*(2, \bar{P}; \mathcal{S}_B, \mathcal{N}_{AB}^{\gamma'}) = 1 - \frac{3}{4}\gamma'. \quad (\text{G.6})$$

Here, we have that the optimal PPT purification protocol is trivial. Note that the LOCC is a subset of the PPT operations; we directly have the optimal LOCC purification protocol is trivial, implying no nontrivial LOCC protocol can purify four orthogonal maximally entangled states. The proof is completed. ■

Supplemental Material H: Proof of Theorem 5

We divide the proof of Theorem 5 into two parts. In the first part, we show that the protocol shown in FIG. 6 could purify the quantum states in the form of $|\psi_\alpha\rangle = \alpha|00\rangle + \sqrt{1-\alpha^2}|11\rangle$ corrupted by local depolarizing noise $\mathcal{N}_{AB}^{\gamma,\gamma} = \mathcal{N}_A^\gamma \otimes \mathcal{N}_B^\gamma$, where $\alpha \in [0, 1]$, $\beta = \sqrt{1-\alpha^2}$ (Lemma 10). Specifically, Alice and Bob possess two copies of shared local depolarizing noisy states $\mathcal{N}_{AB}^{\gamma,\gamma}(\psi_\alpha)$; they apply RX gates and CNOT gates on their own systems. Then, Alice and Bob make measurements on systems A_2, B_2 and denote the measurement results as m_A and m_B , respectively. Then they exchange the results via classical communication. If $m_A = m_B = 0$, then the purification is successful and outputs the purified state σ_ψ ; Otherwise, the purification fails, and the process needs to be repeated.

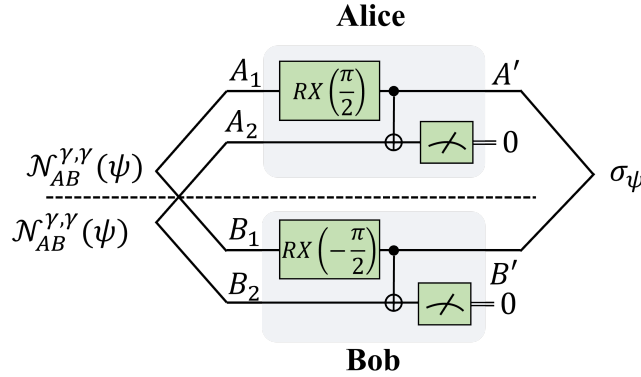


FIG. 6. $2 \rightarrow 1$ purification protocol for noisy state $\mathcal{N}_{AB}^{\gamma,\gamma}(\psi_\alpha)$, where $|\psi_\alpha\rangle = \alpha|00\rangle + \sqrt{1-\alpha^2}|11\rangle$. Alice and Bob apply RX and CNOT gates on their own part, respectively. Then both parties make measurements on the second registers, and exchange the measurement results. If the measurements are '00', then the purification is successful; Otherwise, the purification fails and needs to repeat the processes.

Lemma 10 *If the quantum state in the form $|\psi_\alpha\rangle = \alpha|00\rangle + \sqrt{1-\alpha^2}|11\rangle$ with $\alpha \in [0, 1]$, the proposed protocol is a nontrivial $2 \rightarrow 1$ distribute purification protocol \mathcal{E} such that $F(\psi_\alpha, \mathcal{N}_{AB}^{\gamma,\gamma}(\psi_\alpha)) \leq F(\psi_\alpha, \mathcal{E}(\mathcal{N}_{AB}^{\gamma,\gamma}(\psi_\alpha)^{\otimes 2}))$, where $\mathcal{N}_{AB}^{\gamma,\gamma}$ is the local depolarizing noise with noise level $\gamma \in [0, 0.4]$.*

Proof Here we will prove that the fidelity between the target state $|\psi_\alpha\rangle = \alpha|00\rangle + \beta|11\rangle$ and the purified state $\mathcal{E}(\mathcal{N}_{AB}^{\gamma,\gamma}(\psi_\alpha)^{\otimes 2})$, where \mathcal{E} is the proposed $2 \rightarrow 1$ is larger than no-purification fidelity. In other words, the aim is to prove

$$F(\psi_\alpha, \mathcal{E}(\mathcal{N}_{AB}^{\gamma,\gamma}(\psi_\alpha)^{\otimes 2})) - F(\psi_\alpha, \mathcal{N}_{AB}^{\gamma,\gamma}(\psi_\alpha)) \geq 0. \quad (\text{H.1})$$

By applying the protocol \mathcal{E} proposed in FIG. 6, the increased fidelity can be calculated, thus our aim becomes to prove

$$F(\psi_\alpha, \mathcal{E}(\mathcal{N}_{AB}^{\gamma,\gamma}(\psi_\alpha)^{\otimes 2})) - F(\psi_\alpha, \mathcal{N}_{AB}^{\gamma,\gamma}(\psi_\alpha)) = \frac{f(\alpha, \gamma)g(\alpha, \gamma)}{d(\alpha, \gamma)} \geq 0, \quad (\text{H.2})$$

where

$$d(\alpha, \gamma) = 2(1 + 2\alpha\sqrt{1-\alpha^2}(\gamma-1)^4), \quad (\text{H.3})$$

$$f(\alpha, \gamma) = \alpha\gamma(\gamma - 2)(\gamma - 1)^2, \quad (\text{H.4})$$

$$g(\alpha, \gamma) = 4\alpha - 4\alpha^3 - \sqrt{1 - \alpha^2}(\gamma - 2)^2 + 8\alpha^2\sqrt{1 - \alpha^2}\gamma(\gamma - 1)(\alpha^2 - 1). \quad (\text{H.5})$$

Since $\alpha \in [0, 1]$ and $\gamma \in [0, 0.4]$, we can easily arrive at $d(\alpha, \gamma) > 0$ and $f(\alpha, \gamma) \leq 0$. Now, we need to prove $g(\alpha, \gamma) \leq 0$. Fix the variable α and take the derivative over γ , which is

$$\frac{\partial g(\alpha, \gamma)}{\partial \gamma} = \sqrt{1 - \alpha^2}[4 - 2\gamma + 8\alpha^2(\alpha^2 - 1)(2\gamma - 1)]. \quad (\text{H.6})$$

Due to the domain of γ and α , we directly have $\frac{\partial g(\alpha, \gamma)}{\partial \gamma} \geq 0$, which implies the function $g(\alpha, \gamma)$ increase with respect to the increase of γ . Thus, the max value of the function $g(\alpha, \gamma)$ is achieved when $\gamma = 0.4$. If the largest value of $g(\alpha, \gamma)$ is no larger than 0, then the proof is finished. Here, the problem becomes proving

$$g(\alpha, 0.4) = -\frac{4}{25}(25\alpha(\alpha^2 - 1) + \sqrt{1 - \alpha^2}(12\alpha^4 - 12\alpha^2 + 16)) \leq 0. \quad (\text{H.7})$$

It is equivalent to proving

$$k(\alpha) = 25\alpha(\alpha^2 - 1) + \sqrt{1 - \alpha^2}(12\alpha^4 - 12\alpha^2 + 16) \geq 0. \quad (\text{H.8})$$

Consider the end points $k(0) = 16$, $k(1) = 0$. Consider $\alpha \in (0, 1)$, we need to prove

$$25\alpha(\alpha^2 - 1) + \sqrt{1 - \alpha^2}(12\alpha^4 - 12\alpha^2 + 16) \geq 0, \quad (\text{H.9})$$

$$\sqrt{1 - \alpha^2}(12\alpha^4 - 12\alpha^2 + 16) \geq 25\alpha(1 - \alpha^2). \quad (\text{H.10})$$

Since $25\alpha(1 - \alpha^2) > 0$ and $\sqrt{1 - \alpha^2}(12\alpha^4 - 12\alpha^2 + 16) > 0$, we can take square on both side

$$[\sqrt{1 - \alpha^2}(12\alpha^4 - 12\alpha^2 + 16)]^2 \geq [25\alpha(1 - \alpha^2)]^2. \quad (\text{H.11})$$

Note that $1 - \alpha^2 \geq 0$, we can reduce it to

$$(12\alpha^4 - 12\alpha^2 + 16)^2 \geq 625\alpha^2(1 - \alpha^2). \quad (\text{H.12})$$

Let's $u = \alpha^2 \in (0, 1)$, and define the a function $p(u) = (12u^2 - 12u + 16)^2 - 625u(1 - u)$. Now, our aim becomes to prove $p(u) \geq 0$ for $u \in (0, 1)$. By taking the first and second derivatives of $p(u)$, we found that $u = 0.5$ is the only root for $p'(u)$, implying the minimum value for $p(u)$ is $p(0.5) = 12.75 > 0$. Thus, $p(u) \geq 0$, $u \in (0, 1)$, which implies $g(\alpha, \gamma) \leq 0$. Together with $d(\alpha, \gamma) > 0$ and $f(\alpha, \gamma) \leq 0$, we arrive at

$$F(\psi_\alpha, \mathcal{E}(\mathcal{N}_{AB}^{\gamma, \gamma}(\psi_\alpha))^{\otimes 2}) - F(\psi_\alpha, \mathcal{N}_{AB}^{\gamma, \gamma}(\psi_\alpha)) = \frac{f(\alpha, \gamma)g(\alpha, \gamma)}{d(\alpha, \gamma)} \geq 0. \quad (\text{H.13})$$

The proof is complete. ■

In the second part, we are going to prove that an arbitrary bipartite pure state $|\psi\rangle$ is equivalent to the $|\psi_\alpha\rangle$ up to the local unitaries, i.e., $\exists U, V, \alpha$ such that $|\psi\rangle = U \otimes V |\psi_\alpha\rangle$. Then we can transfer the state into the form of $|\psi_\alpha\rangle$ via local unitaries first, and then we can apply the protocol shown in FIG. 6 can be used to purify the noisy state.

Theorem 5 (Go theorem for arbitrary state) *For the local depolarizing noise channel $\mathcal{N}_{AB}^{\gamma, \gamma}$ with noise level $\gamma \in [0, 0.4]$, the proposed $2 \rightarrow 1$ analytical distributed purification protocol is nontrivial for arbitrary pure states.*

Proof For arbitrary given state $|\psi\rangle$, which can represent it in the Schmidt decomposition form $|\psi\rangle = \alpha|u_1\rangle_A|v_1\rangle_B + \beta|u_2\rangle_A|v_2\rangle_B$, the protocol $\mathcal{U}^\dagger \circ \mathcal{E} \circ \mathcal{U}^{\otimes 2}(\cdot)$ is a nontrivial distributed purification protocol over the local depolarizing noisy states, where \mathcal{E} is the protocol shown in FIG. 6, and $\mathcal{U}(\cdot) = U_A \otimes U_B(\cdot)U_A^\dagger \otimes U_B^\dagger$ is unitary channel which maps the state to the form of $\alpha|00\rangle + \beta|11\rangle$ with $U_1 = |0\rangle\langle u_1| + |1\rangle\langle u_2|$ and $U_2 = |0\rangle\langle v_1| + |1\rangle\langle v_2|$. The fidelity between the purified state and the target state is

$$F(\psi, \mathcal{U}^\dagger \circ \mathcal{E} \circ \mathcal{U}^{\otimes 2}(\mathcal{N}_{AB}^{\gamma, \gamma}(\psi)^{\otimes 2})) = \text{Tr}[\psi \mathcal{U}^\dagger \circ \mathcal{E} \mathcal{U}^{\otimes 2}(\mathcal{N}_{AB}^{\gamma, \gamma}(\psi)^{\otimes 2})] \quad (\text{H.14})$$

$$= \text{Tr}[\psi U_A^\dagger \otimes U_B^\dagger \mathcal{E}[U_A^{\otimes 2} \otimes U_B^{\otimes 2}(\mathcal{N}_{AB}^{\gamma, \gamma}(\psi)^{\otimes 2})U_A^{\otimes 2\dagger} \otimes U_B^{\otimes 2\dagger}]U_A \otimes U_B] \quad (\text{H.15})$$

$$= \text{Tr}[U_A \otimes U_B \psi U_A^\dagger \otimes U_B^\dagger \mathcal{E}[U_A^{\otimes 2} \otimes U_B^{\otimes 2} (\mathcal{N}_{AB}^{\gamma, \gamma}(\psi)^{\otimes 2}) U_A^{\otimes 2 \dagger} \otimes U_B^{\otimes 2 \dagger}]]. \quad (\text{H.16})$$

Note that the depolarizing channel commutes with local unitary,

$$U \cdot \mathcal{N}^\gamma(\psi) \cdot U^\dagger = U \cdot [(1 - \gamma)\psi + \gamma \frac{I}{d}] \cdot U^\dagger = (1 - \gamma)U\psi U^\dagger + \gamma \frac{I}{d} \quad (\text{H.17})$$

$$= \mathcal{N}^\gamma(U\psi U^\dagger). \quad (\text{H.18})$$

Thus, the fidelity becomes

$$F(\psi, \mathcal{U}^\dagger \circ \mathcal{E} \circ \mathcal{U}^{\otimes 2}(\mathcal{N}_{AB}^{\gamma, \gamma}(\psi)^{\otimes 2})) = \text{Tr}[U_A \otimes U_B \psi U_A^\dagger \otimes U_B^\dagger \mathcal{E}[U_A^{\otimes 2} \otimes U_B^{\otimes 2} (\mathcal{N}_{AB}^{\gamma, \gamma}(\psi)^{\otimes 2}) U_A^{\otimes 2 \dagger} \otimes U_B^{\otimes 2 \dagger}]] \quad (\text{H.19})$$

$$= \text{Tr}[U_A \otimes U_B \psi U_A^\dagger \otimes U_B^\dagger \mathcal{E}[(\mathcal{N}_{AB}^{\gamma, \gamma}(U_A \otimes U_B \psi U_A^\dagger \otimes U_B^\dagger)^{\otimes 2})]] \quad (\text{H.20})$$

$$= \text{Tr}[\psi' \mathcal{E}[(\mathcal{N}_{AB}^{\gamma, \gamma}(\psi')^{\otimes 2})]] \quad (\text{H.21})$$

$$= F(\psi', \mathcal{E}(\mathcal{N}_{AB}^{\gamma, \gamma}(\psi')^{\otimes 2})), \quad (\text{H.22})$$

where $\psi' = U_A \otimes U_B \psi U_A^\dagger \otimes U_B^\dagger = \alpha|00\rangle + \beta|11\rangle$. According to Lemma 10, we directly arrive at

$$F(\psi, \mathcal{U}^\dagger \circ \mathcal{E} \circ \mathcal{U}^{\otimes 2}(\mathcal{N}_{AB}^{\gamma, \gamma}(\psi)^{\otimes 2})) = F(\psi', \mathcal{E}(\mathcal{N}_{AB}^{\gamma, \gamma}(\psi')^{\otimes 2})) \quad (\text{H.23})$$

$$\geq F(\psi', \mathcal{N}_{AB}^{\gamma, \gamma}(\psi')) = F(\psi, \mathcal{N}_{AB}^{\gamma, \gamma}(\psi)). \quad (\text{H.24})$$

The proof is complete. ■

Supplemental Material I: Optimized purification protocol

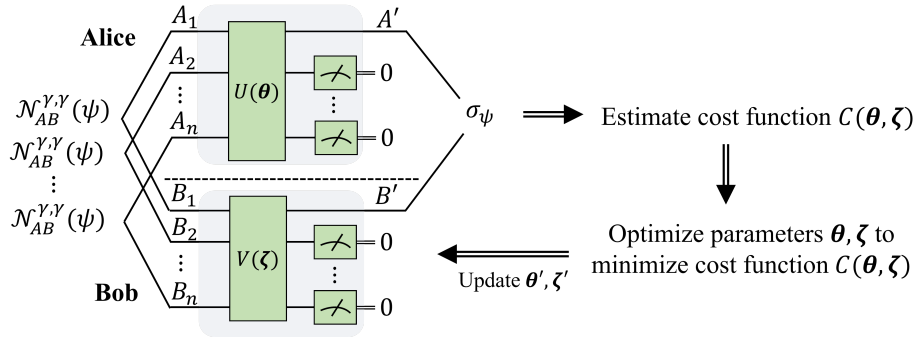


FIG. 7. Framework of the optimization purification algorithm. Alice and Bob apply local unitaries $U(\theta)$ and $V(\zeta)$ on their systems, respectively. Then they make measurements on the systems and check the measurement results via classical communication. If the results are all 0, then output the purified state σ_ψ ; otherwise, repeat the process until it succeeds. With the purified state σ_ψ , we can estimate the cost function $C(\theta, \zeta)$. The cost function can be minimized by utilizing a classical optimizer, updating the parameters to the PQCs, and repeating the iterations until the cost function converges to its minimum.

Note that the success case can be defined flexibly. For example, one can define the success case as measurements of ancillary systems are all 1 or all 0. In our case, we only define the measurement as all 0 as the successful case. The algorithm may achieve higher fidelity by introducing ancilla qubits.

The choice of the unitary ansatz should be made carefully, for the trade-off between trainability and expressibility. If the ansatz we choose is very complex and the number of parameters is large, it may express more quantum states. However, at the same time, it will be harder to train, preventing us from achieving the optimal result. On the contrary, if the ansatz is simple and the number of parameters is small, then it is very easy to train. But the global optimal results may not be expressed by the ansatz. Meanwhile, the barren plateaus, referring to a phenomenon in which the gradient decreases exponentially with respect to the increase of quantum system size, is another important problem we have to take into consideration. Choosing a suitable quantum ansatz and setting the starting parameters carefully can also circumvent barren plateaus to some extent [71, 72]. As we focus on the $2 \rightarrow 1$ purification protocol, we choose the ansatz as *universal 2-qubit gate* [73, 74], which can represent an arbitrary 2-qubit unitary with 15 parameters.

Algorithm 1: Optimization algorithm for designing a distributed purification protocol

Input: Noisy state $\mathcal{N}(\psi)$ with ψ is sampled from the state \mathcal{S} , two parameterized quantum circuits (PQC) $U(\theta)$ and $V(\zeta)$, number of iterations ITR,

Output: Quantum circuit for LOCC purification protocol $U(\theta^*) \otimes V(\zeta^*)$

- 1: Randomly initialize parameters θ, ζ , and prepare the circuit ansatz $U(\theta), V(\zeta)$
- 2: **for** itr = 1, . . . , ITR **do**
- 3: **for** state $\psi \in \mathcal{S}$ **do**
- 4: Apply $U(\theta)$ and $V(\zeta)$ to the noisy states $\mathcal{N}(\psi)^{\otimes n}$
- 5: Make measurements on the ancillary qubit
- 6: **if** Measurement results are all 0 **then**
- 7: The purification is successful and outputs the purified state σ_ψ
- 8: **else**
- 9: Repeat the process until it succeeds.
- 10: **end if**
- 11: Compute the fidelity $F(\psi, \sigma_\psi)$
- 12: **end for**
- 13: Estimate the cost function $C(\theta, \zeta)$ as shown in Eq. (4)
- 14: Minimize the cost function C and update parameter θ', ζ' via classical computers
- 15: **end for**
- 16: Output the optimized circuit for distributed purification protocol $U(\theta^*) \otimes V(\zeta^*)$

Supplemental Material J: Distributed purification protocol for the set \mathcal{S}_d with extended noise levels

In the numerical experiments shown in FIG. 3, we consider the pure state set containing 4 different states $\mathcal{S}_d = \{\psi_{\frac{1}{\sqrt{2}}}, \psi_{\frac{1}{\sqrt{3}}}, \psi_{\frac{1}{\sqrt{4}}}, \psi_{\frac{1}{\sqrt{5}}}\}$, where $|\psi_\alpha\rangle = \alpha|00\rangle + \sqrt{1-\alpha^2}|11\rangle$. The noise model is bi-local depolarizing channel $\mathcal{N}_{AB}^{\gamma, \gamma}$, with noise level varying $\gamma \in [0, 0.4]$. However, if we extend the noise level γ to 0.5, the behavior of the PPT bound becomes complicated. The numerical experiments are conducted, and the results are shown in Fig. 8. One can observe that the PPT bound jumps around $\gamma \approx 0.43$, and then the average fidelity remains at 0.71 as the noise level increases. It is natural to ask the following two questions:

- **Question:** Why there is a jump point around 0.43?

Answer: When $\gamma \geq 0.43$, if the purification protocol is successful, the corresponding operation is the replacement channel, which maps any input state to the a fixed state, i.e., $\frac{\mathcal{E}(\mathcal{N}(\rho) \otimes \mathcal{N}(\rho))}{\text{Tr}[\mathcal{E}(\mathcal{N}(\rho) \otimes \mathcal{N}(\rho))]} = |11\rangle\langle 11|$ (We call it replacement protocol for convenience in the following). Set the noise level as $\gamma = 0.43$. Before purification, the fidelities $F(\mathcal{N}(\psi_\alpha), \psi_\alpha)$ of the state set \mathcal{S}_d are $\{0.4937, 0.5073, 0.5243, 0.5378\}$, respectively, while the purified state fidelity $F(\sigma_{\psi_\alpha}, \psi_\alpha)$ becomes $\{0.5, 0.6667, 0.75, 0.8\}$, where σ_{ψ_α} refers to the purified state. By the definition of purification protocol, for any state in the set, the purified state should have a larger fidelity, i.e.,

$$F(\sigma_\psi, \psi) \geq F(\mathcal{N}(\psi), \psi), \quad \forall \psi \in \mathcal{S}_d. \quad (\text{J.1})$$

Therefore, the replacement protocol is a valid purification protocol. The optimal purified average fidelity is calculated by

$$\bar{F} = \sum_{\alpha} p_{\alpha} F(\sigma_{\psi_{\alpha}}, \psi_{\alpha}), \quad (\text{J.2})$$

with $\sum_{\alpha} p_{\alpha}/4 = \bar{P} = 0.1$. By SDP, the success probabilities p_{α} are given by $\{0.0569, 0.0941, 0.1169, 0.1321\}$, and the optimal average fidelity is calculated to be $\bar{F} = 0.7113$.

However, when $\gamma \leq 0.42$, the replacement protocol shown above is no longer feasible. For example, let's take $\gamma = 0.42$, the fidelities before purification are $\{0.5023, 0.5158, 0.5327, 0.5461\}$, respectively. Clearly, if we apply the PPT purification protocol directly, the fidelity of the first output state drops, i.e.,

$$F(\sigma_{\psi_{\frac{1}{\sqrt{2}}}}, \psi_{\frac{1}{\sqrt{2}}}) = 0.5 < 0.5023 = F(\mathcal{N}(\psi_{\frac{1}{\sqrt{2}}}), \psi_{\frac{1}{\sqrt{2}}}), \quad (\text{J.3})$$

which contradicts the definition of the purification protocol, i.e., the replacement protocol is not feasible for $\gamma = 0.42$. That's why there is a jump around $\gamma = 0.43$.

- **Question:** Why cannot the optimization method converge to the replacement protocol as PPT does?

Answer: The replacement channel is basically a measure-and-prepare operation. The ansatz we used in the optimization algorithm can only optimize LOCC protocols consisting of local unitaries; the measure-and-prepare operation is outside the scope of the chosen ansatz. If we apply other kinds of ansatz, e.g., with ancilla systems and partial trace operation, it is possible for the optimized protocol to converge to the replacement protocol.

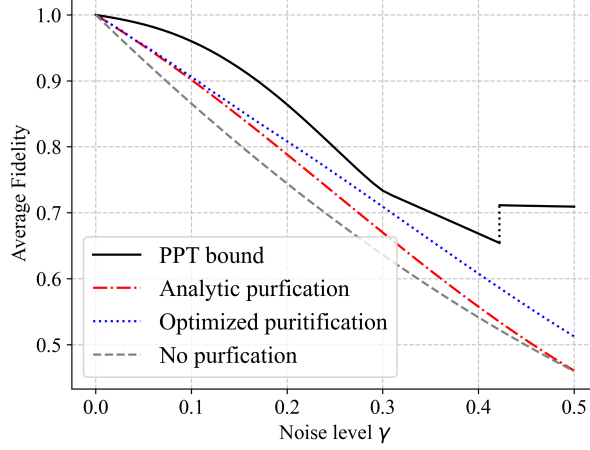


FIG. 8. Performance of $2 \rightarrow 1$ purification with different strategies for the set \mathcal{S}_d over bi-local depolarizing noise with noise level $\gamma \in [0, 0.5]$.

Note that a similar fidelity jump is also observed in the purification of the set \mathcal{S}_d degraded by the mixed Pauli noise channel $\mathcal{N}_{\text{Pauli}}^\gamma \otimes \mathcal{N}_{\text{Pauli}}^\gamma$, where

$$\mathcal{N}_{\text{Pauli}}^\gamma(\rho) = (1 - \gamma)\rho + \frac{\gamma}{2}X\rho X + \frac{\gamma}{4}Y\rho Y + \frac{\gamma}{4}Z\rho Z. \quad (\text{J.4})$$

The PPT bound for the $2 \rightarrow 1$ protocol is shown in FIG. 9.

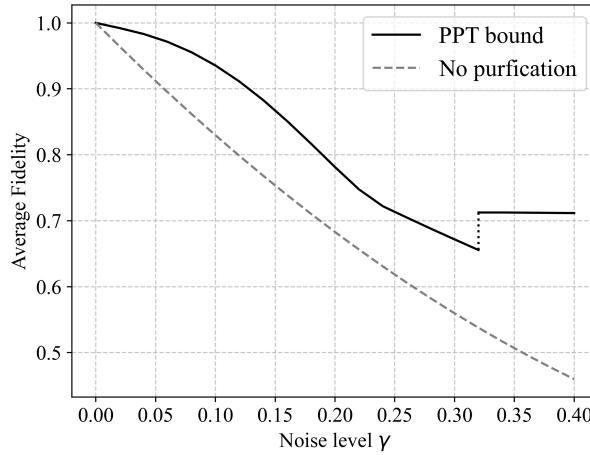


FIG. 9. Performance of $2 \rightarrow 1$ purification with different strategies for the set \mathcal{S}_d over mixed Pauli noise $\mathcal{N}_{\text{Pauli}}^\gamma \otimes \mathcal{N}_{\text{Pauli}}^\gamma$.

However, the jump point does not always exist. It is highly dependent on the state set and the quantum noise. For example, if the set is the four Bell states, i.e., \mathcal{S}_B , and the quantum noise is amplitude damping noise, then there is no such jump point, as illustrated in FIG. 10.

Supplemental Material K: Additional numerical results

In the main text, we only consider purifying the depolarizing noise corrupted states with $2 \rightarrow 1$ LOCC purification protocols. However, the tools proposed in this work, such as the SDP for the bound of purification and the protocol design with an optimization-based method, can be applied to a more general scenario. Here, we conduct more numerical experiments to demonstrate the power of tools utilized in this work.

1. $2 \rightarrow 1$ LOCC purification protocol for sets with Bell states

Here, we consider 4 different state sets which contain 4, 3, 2, and 1 Bell states respectively, i.e., $\mathcal{S}_{B_4} = \{\Phi^+, \Phi^-, \Psi^+, \Psi^-\}$, $\mathcal{S}_{B_3} = \{\Phi^+, \Phi^-, \Psi^+\}$, $\mathcal{S}_{B_2} = \{\Phi^+, \Psi^+\}$, and $\mathcal{S}_{B_1} = \{\Phi^+\}$. The noise we consider is a bi-local depolarizing noise model. The numerical results are shown in TABLE I. In this table, ‘‘No Pure’’ refers to the averaged fidelity between the noised state and target state, i.e., $\frac{1}{|\mathcal{S}|} \sum_{\psi \in \mathcal{S}} F(\mathcal{N}(\psi), \psi)$. The ‘‘PPT Bound’’ is computed via the SDP given in Eq. (E.2) with the average successful probability $\bar{P} = 0.1$. The ‘‘Optimized’’ refers to the averaged fidelity computed by the protocols, which are designed by the proposed optimization-based method as shown in Algorithm 1.

The numerical results demonstrate the following:

- For bi-local depolarizing noise $\mathcal{N}_{DE}^\gamma \otimes \mathcal{N}_{DE}^\gamma$ with noise level $\gamma \in [0, 0.4]$, there is no non-trivial $2 \rightarrow 1$ LOCC purification protocol for the set with three or four Bell states, i.e., \mathcal{S}_{B_3} and \mathcal{S}_{B_4} .
- For bi-local depolarizing noise $\mathcal{N}_{DE}^\gamma \otimes \mathcal{N}_{DE}^\gamma$ with noise level $\gamma \in [0, 0.4]$, there exists a non-trivial $2 \rightarrow 1$ LOCC purification protocol for the set with two or one Bell states, i.e., \mathcal{S}_{B_2} and \mathcal{S}_{B_1} .
- For the set with two Bell states, i.e., \mathcal{S}_{B_2} , the protocol designed by the optimization-based method is near-optimal as the fidelity achieved by the optimized protocol is very close to the PPT bound.

These conclusions shown here are inferred from numerical results. Rigorous proofs are necessary to make them solid.

Noise Level γ	\mathcal{S}_{B_1}			\mathcal{S}_{B_2}			\mathcal{S}_{B_3}		\mathcal{S}_{B_4}	
	No Pure	PPT Bound	Optimized	No Pure	PPT Bound	Optimized	No Pure	PPT Bound	No Pure	PPT Bound
0	1.0	1.0	1.0	1.0	1.0	1.0	1.0	1.0	1.0	1.0
0.1	0.8575	0.9731	0.8907	0.8575	0.8907	0.8907	0.8575	0.8575	0.8575	0.8575
0.2	0.7300	0.8797	0.76759	0.7300	0.7676	0.76759	0.7300	0.7300	0.7300	0.7300
0.3	0.6175	0.7227	0.64118	0.6175	0.6412	0.64117	0.6175	0.6175	0.6175	0.6175
0.4	0.5200	0.5399	0.5241	0.5200	0.5241	0.5241	0.5200	0.5200	0.5200	0.5200

TABLE I. State purification for the sets with Bell states.

2. $2 \rightarrow 1$ LOCC purification protocol for Bell set \mathcal{S}_B over other noise models

Here, we conduct another numerical experiment to show the performance of state purification for the Bell set $\mathcal{S}_B = \{\Phi^\pm, \Psi^\pm\}$ over the bi-local amplitude damping noise $\mathcal{N}_{AD}^\gamma \otimes \mathcal{N}_{AD}^\gamma$. The Amplitude damping noise \mathcal{N}_{AD}^γ is particularly relevant for the loss of energy or the dissipation of excited states, which is characterized by the damping rate γ , and has two Kraus operators:

$$A_0^\gamma = |0\rangle\langle 0| + \sqrt{1-\gamma}|1\rangle\langle 1|, \quad A_1^\gamma = \sqrt{\gamma}|0\rangle\langle 1| \quad (\text{K.1})$$

The numerical results are shown in FIG. 10. The PPT bound is computed via the SDP given in Eq. (E.2) with the average successful probability $\bar{P} = 0.1$. The optimized purification refers to the averaged fidelity computed by the protocols, which are designed by the proposed optimization-based method as shown in Algorithm 1. From the numerical results, we observe that for bi-local amplitude damping noise, unlike depolarizing noise, it is possible to purify the set with four Bell states via state purification.

We also take bi-local dephasing noise $\mathcal{N}_{DP}^\gamma \otimes \mathcal{N}_{DP}^\gamma$ into consideration, which probabilistically applies the Pauli-Z operation on the quantum state, i.e.,

$$\mathcal{N}_{DP}^\gamma(\rho) = (1-\gamma)\rho + \gamma Z\rho Z. \quad (\text{K.2})$$

From the SDP numerical results, the optimal blind purification protocol cannot increase the fidelity at all, as shown in Table II. Therefore, for the bi-local dephasing noise, there is no non-trivial LOCC (even PPT) $2 \rightarrow 1$ state purification protocol for the set with four Bell states \mathcal{S}_B .

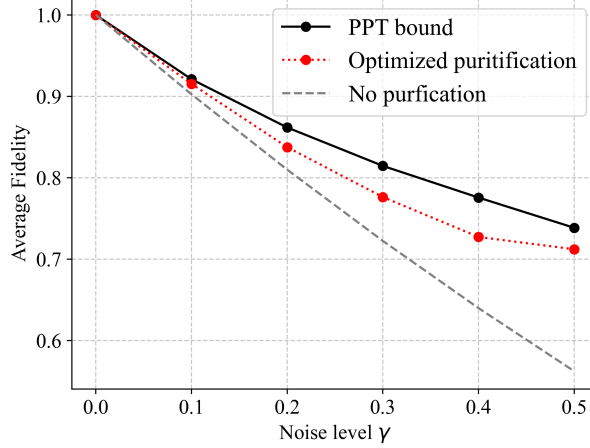


FIG. 10. State purification for bi-local amplitude damping corrupted Bell set \mathcal{S}_B .

Noise level γ	0	0.1	0.2	0.3	0.4	0.5
No purification	1.000	0.905	0.820	0.745	0.680	0.625
PPT bound	1.000	0.905	0.820	0.745	0.680	0.625

TABLE II. The PPT bound of purification for Bell set \mathcal{S}_B over the bi-local dephasing noise.

3. Comparison between optimized protocol and DEJMPS protocol

To benchmark the performance of the optimized protocol, it is natural to make a comparison with conventional methods, such as DEJMPS [42] and BBPSSW [14]. Note that DEJMPS works on a broader set of states than BBPSSW. Therefore, we conduct numerical experiments with different settings to compare our protocol with DEJMPS.

- First, we consider the purification of the canonical maximally entangled state Φ^+ , degraded by bi-depolarizing noise $\mathcal{N}_{DE}^\gamma \otimes \mathcal{N}_{DE}^\gamma$ into a Bell-diagonal state. Here, we also conduct a numerical experiment to compare the protocol designed by the optimization-based method and the well-known DEJMPS protocol [42]. The results are shown in TABLE III. The optimized protocol achieves the same fidelity as the DEJMPS protocol, implying the power of the proposed optimization-based method.

Noise level	0.1	0.2	0.3	0.4
No purification	0.8575	0.7300	0.6175	0.5200
DEJMPS protocol	0.8907	0.7676	0.6412	0.5241
Optimized protocol	0.8907	0.7676	0.6412	0.5241

TABLE III. Comparison between the $2 \rightarrow 1$ optimized purification protocol and the DEJMPS protocol over bi-depolarizing noise.

- Second, we consider the purification of the maximally entangled state Φ^+ degraded by amplitude damping noise applied on both sides, i.e., $\mathcal{N}_{AD}^\gamma \otimes \mathcal{N}_{AD}^\gamma$. In this case, from the numerical results shown in Fig. 11 (a), our optimized protocol outperforms DEJMPS. This result could be expected, because DEJMPS is tailored to Bell diagonal states, whereas the output of the amplitude damping channels is not Bell diagonal anymore.
- Finally, we consider an example involving the purification of more than a single maximally entangled state. Specifically, we choose the three maximally entangled states $\{\Phi^+, U_1 \otimes I(\Phi^+)U_1^\dagger \otimes I, U_2 \otimes I(\Phi^+)U_2^\dagger \otimes I\}$, where U_1 and U_2 are X -rotation gates with rotation angles 0.2 and -0.2, respectively, i.e., $U_1 = RX(0.2)$ and $U_2 = RX(-0.2)$. These three states are degraded by depolarizing noise applied to both systems. The results are shown in Fig. 11 (b). In this case, our protocol also outperforms DEJMPS. Again, this finding is no surprise, because the task is to purify a set of maximally entangled states simultaneously, rather than just purify the canonical maximally entangled state, and therefore is outside the scope for which DEJMPS was designed.

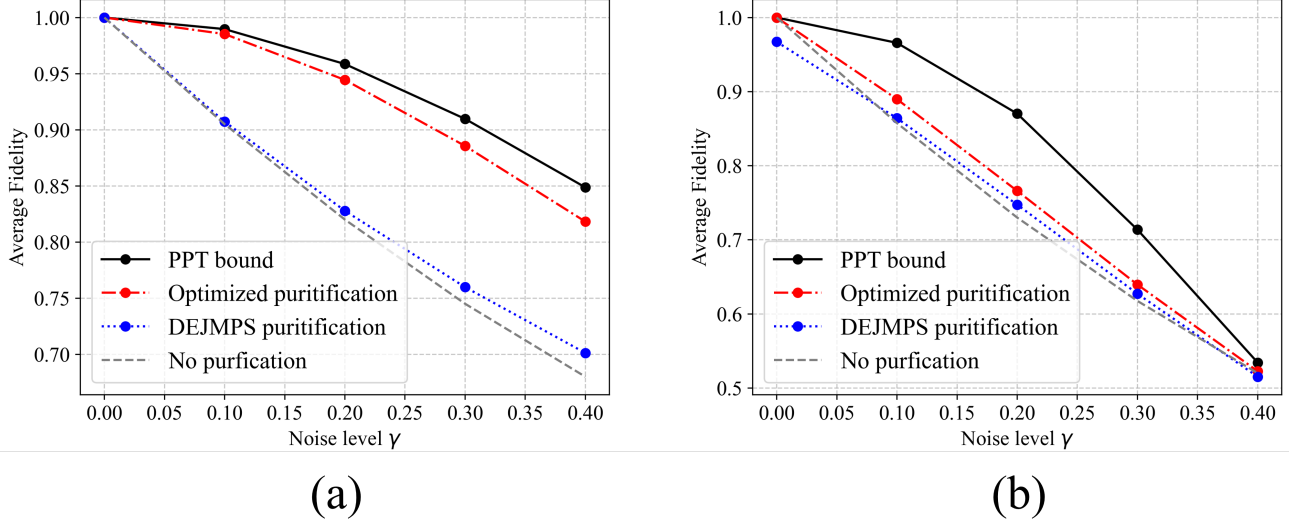


FIG. 11. The comparison between the $2 \rightarrow 1$ optimized purification protocol and the DEJMPS protocol. (a) The input state is Bell states corrupted by amplitude damping noise $\mathcal{N}_{AD}^\gamma \otimes \mathcal{N}_{AD}^\gamma(\Phi^+)$. (b) The input states are sampled from the depolarized maximally entangled state set $\Phi^+, U_1 \otimes I(\Phi^+)U_1^\dagger \otimes I, U_2 \otimes I(\Phi^+)U_2^\dagger \otimes I$, where U_1, U_2 are rotation-X operations with rotation angle 0.2 and -0.2, respectively.

4. $3 \rightarrow 1$ LOCC purification protocol for the set \mathcal{S}_d over depolarizing noise

The purification protocol via optimization proposed in Algorithm 1 is actually valid for the $n \rightarrow 1$ case. In the main text, we only show the performance of $2 \rightarrow 1$ protocols. Here, conduct another numerical experiment to show the performance of $3 \rightarrow 1$ LOCC purification protocol. The state set we choose is $\mathcal{S}_d = \{\psi_{\frac{1}{2}}, \psi_{\frac{1}{3}}, \psi_{\frac{1}{4}}, \psi_{\frac{1}{5}}\}$, and noise is bi-local depolarizing noise $\mathcal{N}_{DE}^\gamma \otimes \mathcal{N}_{DE}^\gamma$.

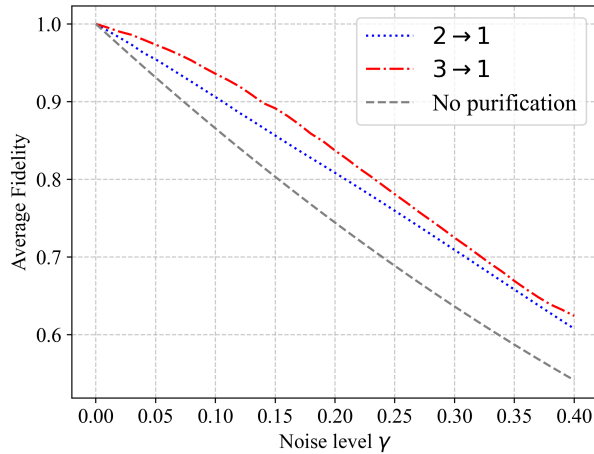


FIG. 12. The performance comparison between $2 \rightarrow 1$ and $3 \rightarrow 1$ purification protocols.

From the numerical results shown in FIG. 12, the $3 \rightarrow 1$ protocol outperforms the $2 \rightarrow 1$ protocol, which is an intuitive result as $3 \rightarrow 1$ protocol consumes more resources. Theoretically, the more copies that are consumed in the purification protocol, the higher the fidelity that will be achieved. Of course, meanwhile, it is becoming harder to train the protocol via the optimization-based method.